Treatment of anti-myeloperoxidase glomerulonephritis using recombinant deoxyribonuclease I is enhanced by adeno-associated virus gene therapy

Anne Cao Le[1]

Poh-Yi Gan[1]

Daniel Koo Yuk Cheong[1]

Virginie Oudin[1]

Jonathan Dick[1]

Maliha A. Alikhan[1]

Mawj Mandwie[2]

Ian E Alexander[2,3]

A. Richard Kitching[1,4]

Grant J Logan[2¥]

Kim M O'Sullivan[1*¥]

[1]Centre for Inflammatory Diseases, Monash University Department of Medicine, 246 Clayton Rd, Clayton, VIC 3168, Australia

[2]Gene Therapy Research Unit, Children's Medical Research Institute and Sydney Children's Hospitals Network, University of Sydney, Westmead, New South Wales, Australia

[3]Discipline of Child and Adolescent Health, University of Sydney, Westmead, Australia.

[4]Department of Nephrology, Monash Health, 246 Clayton Rd, Clayton VIC 3168, Australia

[¥]Grant J Logan and Kim M O'Sullivan contributed equally to this manuscript

Running title: Deoxyribonuclease to remove ecDNA and treat MPO-AAV

Correspondence: *****Dr Kim Maree O'Sullivan, Centre for Inflammatory Diseases, Monash University, Department of Medicine, Monash Medical Centre, 246 Clayton Road, Clayton, VIC 3168, Australia

Phone: +61 3 85722090 **Fax:** +61 9594 6495

Email: kim.osullivan@monash.edu

Words: Word limit is 12000, 9000 minimum Abstract: 196 References: 67

Disclosure: Nothing to disclose

Author contributions:

K.M.O., G.J.L A.R.K, and I.A.E., conceptualized the study, K.M.O., A.C.L., P.Y.G., J.D., M.A.A., M.M., G.J.L., preformed the experiments, K.M.O., A.C.L., P.Y.G., J.D., M.A.A., M.M., G.J.L., analyzed the data, K.M.O., wrote the first draft, made the figures, and K.M.O., G.J.L., I.A.E and A.R.K., reviewed and edited the paper, K.M.O and G.J.L. acquired the funding, all authors approved the final version of the manuscript.

ABSTRACT

Extracellular DNA (ecDNA) released from injured and dying cells powerfully induces injurious inflammation. In this study we show ecDNA renal presence in patients and experimental mice with myeloperoxidase anti-neutrophil cytoplasmic antibody-associated glomerulonephritis (MPO-ANCA GN). Twice daily administration of intravenous DNase I (ivDNase I) in two models of anti-MPO GN was effective at reducing glomerular deposition of ecDNA, histological injury, leukocyte infiltration and NETosis. Comprehensive investigation into DNase I modes of action revealed the enzyme reduced lymph node DC numbers and their activation status, resulting in decreased frequency of MPO-specific CD4 effector T cells (IFN-γ, and IL17A producing), reductions in dermal anti-MPO delayed type hypersensitivity responses and increased frequency of MPO-specific T regulatory cells. Renal expression of inflammatory chemokines were also decreased. To overcome the translational obstacle of the short half-life of DNase I (<5 hours), we tested an adeno-associated viral vector encoding DNase I in one of the models. Along with the endpoint changes described above, a single vector treatment also enhanced therapeutic benefit as seen by reductions in MPO-ANCA and albuminuria. These results indicate ecDNA is a potent driver of anti-MPO GN and that DNase I is a potential therapeutic that can be delivered using gene technology.

Introduction

Myeloperoxidase (MPO) ANCA-associated glomerulonephritis (GN) left untreated can progress to end-stage renal failure. Current treatment for the disease is non-specific and is associated with detrimental side effects due to broad immunosuppression, which leaves patients highly susceptible to infections (1, 2). Understanding the underlying disease mechanisms of MPO-ANCA GN affords the opportunity to develop new biological therapeutics that target critical components of nephritogenic immune pathways and potentially offer safer more specific treatments.

MPO-ANCA GN has a characteristic pattern of pathological glomerular injury with considerable cell death and necrosis (3-6). Death or injury of large numbers of cells can release pro-inflammatory damage-associated molecular patterns (DAMPs), including nuclear release of DNA as extracellular DNA (ecDNA). DAMP associated ecDNA can be released from different forms of cell death governed by distinct biochemical pathways. Apoptosis which is dependent on caspase releases smaller amounts of ecDNA whereas necroptosis dependent on receptor interacting proteins kinases (RIPK) RIPK1/RIPK3 and the pseudokinase mixed lineage kinase domain-like (MLKL) signaling pathways releases larger sized DNA, however both forms of cell death are characterized by chromatin condensation (7). In contrast, neutrophil extracellular traps (NETs) expel large strands of DNA and is identified through de-condensation of chromatin which relies heavily on reactive oxygen species (ROS) and protein-arginine deiminase 4 (PAD4) dependent citrullination of histones (8-12). NETs are thought to occur to increase the bactericidal killing capacity of neutrophils by extending the surface area in which to entrap bacteria (8, 13). However, in the context of sterile inflammation NETs are highly injurious releasing over 70 known autoantigens (14, 15). Fragments of ecDNA (including CpG oligonucleotides) are a major product of all these forms of cell death and drives inflammatory gene expression. Of particular interest is

detection of ecDNA and signaling through cytosolic and membrane-bound DNA sensors such as Toll like receptor 9 (TLR9), stimulator of interferon genes (STING) and cyclic GMP-AMP synthase (cGAS) as they induce inflammatory responses in sterile inflammation through NFkB nuclear translocation, type 1 interferon cytokine production (IFN-I) and inflammasome activation (12, 16-23) . In host defense, excessive DNA is controlled by endogenous DNase enzymes (24). However, if cellular injury is severe, the production of ecDNA may exceed the capacity for DNase clearance thereby further driving inflammation.

The kidney is a major source of DNase I outside the digestive system and gene deletion of the enzyme in experimental mice induces GN (24-28). These observations support the possibility that DNase I removal of ecDNA is an important physiological process in the renal system. In support of this possibility, sera from patients with acute MPO-ANCA GN have a significant reduction of DNase I and higher levels of serum ecDNA when compared with healthy donors (29). Neutrophil extracellular traps (NETs) occur at high frequency within the glomeruli of patients with MPO-ANCA GN and are a large source of ecDNA (17, 20, 30). Importantly, it has been observed that MPO, the autoantigen in this disease, exerts enhanced biological effects when tethered to the ecDNA in NETs (31). These findings support the notion that ecDNA released from injured and dying glomerular cells and NETosing neutrophils can exceed the capacity for DNase I clearance resulting in ecDNA accumulation in acute disease. The findings also support the possibility that exogenous DNase I administration may restore homeostatic clearance of ecDNA to relieve pathogenic inflammation.

In the current study, we sought to confirm whether ecDNA accumulation occurs in MPO-ANCA GN. We found supporting evidence in the renal biopsies collected from patients with the disease and, additionally, that their renal DNase I expression levels were reduced when compared to control tissues. Similar supporting data for these phenomena was also observed in two murine models of anti-MPO GN where disease is mediated by anti-MPO T cells or

MPO-ANCA. Importantly, intravenous administration of exogenous DNase I (ivDNase I) in the model prevented GN indicating that DNase I is a potential treatment for MPO-ANCA GN. To overcome the translational obstacle of the short half-life of DNase I in serum (<5 hours), we explored the use of DNase I gene transfer using adeno- associated viral vector (AAV) to convert the liver into a bio-factory for enzyme secretion into the circulatory system. The continuous supply of DNase I in the murine anti-MPO-GN model showed enhanced therapeutic efficacy over twice daily doses of ivDNase I, as demonstrated by a significant reduction in MPO-ANCA and albuminuria. Collectively these findings support the pursuit of DNase I for the treatment of MPO-ANCA GN through DNase I gene therapy.

Materials and Methods Sex as a biological variable

MPO-ANCA GN is a disease that equally affects both male and females, therefore both sexes were included in both the biopsy study and mouse studies.

Patient Cohort

29 renal biopsies from consented patients with diagnosed MPO-ANCA GN, and 6 renal biopsies from patients with Minimal Change Disease (MCD) were used in this study (Clinical data in Supplementary Table 1.) Biopsies were collected from 2001-2016 at Monash Health, Clayton, Victoria, Australia. The biopsies from MPO-ANCA GN patients were collected at the patient's first presentation.

Mice

C57BL/6 mice were bred at Monash Medical Centre Animal Facilities and used at 8-10 weeks of age. FcγRIIB-/- mice (C57BL/6J background: B6; 129S-Fcgr2b^{tm1Ttk}/J) were purchased from the Jackson Laboratory (Bar Harbor, ME) and bred at Monash Medical Centre Animal Facilities, Monash University, Australia. The phenotype of FcγRIIB-/- mice was confirmed by flow cytometry with anti-B220 and anti-CD16/CD32Ab (BD Biosciences, North Ryde, NSW, Australia), as previously described (32). Mice aged 8-10 weeks were used for experiments approved by the Monash University Animal Ethics committee (MMCB19/35), under pathogen-free conditions.

Experimental Design

An established model of active anti-MPO autoimmunity was used to assess anti-MPO cell mediated glomerular injury (33-36). WT mice (male and female) were immunized intraperitoneally with 20 µg recombinant murine MPO in Freund's complete adjuvant (FCA; Sigma-Aldrich) and boosted subcutaneously with 10 µg murine MPO in Freund's incomplete

adjuvant (FIA; Sigma- Aldrich) on day. Recombinant murine MPO was isolated and purified as described previously (37).Disease was initiated ('triggered') by intravenous injection of 3mg of anti-GBM on day 16, 4 hours prior to treatment. Anti-MPO autoimmunity and GN was assessed 4 days later (day 20). Non-treated mice received vehicle injections of saline whereas control mice received an irrelevant antigen, OVA instead of MPO. Treated mice received DNase I 10mg/kg (Pulmozyme, Roche, Basel Switzerland) intravenously 4 hours after the last anti-GBM globulin to ensure recruited neutrophils had deposited MPO to initiate disease, and twice daily until termination of the experiment on day 20.

To assess MPO-ANCA (humoral) induced glomerular injury, anti MPO IgG (generated by immunizing *mpo-/-* mice as previously described (38) was passively transferred into *Fcgr2b*$^{-/-}$ mice which are more susceptible to anti-MPO GN (39). Mice were primed by an intraperitoneal injection of LPS (0.5µg/g) 2 hours prior to intravenous transfer of anti-MPO IgG, which activates and recruits neutrophils to glomeruli. DNase I was given intravenously on day -1 and daily until the end of experiments on day 6.

The same 20-day model of anti MPO-GN described above was used for the anti MPO GN AAV8-DNase I experiments, where the both the control GFP vector and DNase I vector were given on day 10 ([intraperitoneal injection of 1 x10^{11} vector genomes (vg per mouse)] and compared to intravenous delivery of recombinant DNase I (Pulomozyme) administered daily from day 16 after triggering of disease with the anti GBM antibody at a concentration of 10mg/kg, until termination of the experiment on day 20.

Adeno associated viral vector production, DNase I activity assay and quantification of liver vector copy number.

Both the GFP control vector and DNase I vector were produced as per our previously published protocol. In brief the vector constructs were subcloned under transcriptional control of a liver

specific promoter (40). Vectors were packaged into an AAV serotype 8 and transfected in HEK-293 cells. At the end of the 20-day anti MPO-GN model livers were removed and examined for vector copy number as previously published (40). Vector copy number was determined using the SuperScript III Reverse Transcriptase kit (Invitro-gen) according to the manufacturer's instructions, using primers specific for the WPRE region on the vector and normalized to GAPDH levels. DNase I activity from plasma samples were determined using radial enzyme diffusion assays according to our previously published protocol (40, 41). The halo diameter around each well of digested DNA was measured and compared to DNase I standards.

Extracellular DNA, Neutrophil extracellular Traps and extracellular MPO detection

To measure extracellular DNA, 3µm FFPE kidney sections were cleared in xylene, rehydrated in graded alcohols, and immersed in antigen retrieval solution (10mM Tris, 1mM EDTA, pH 9.0) and boiled in a pressure cooker for 10 minutes (as described previously)(41). Extracellular DNA was assessed by using colocalization studies using DAPI as a marker for dsDNA [DAPI is nucleic acid specific, which preferentially binds to the AT base pairs in the mirror groove of DNA] and Beta actin as a structural component of all cells to delineate glomerular and cell structures (41). Sections were blocked in 10% Chicken sera in 5% Bovine serum albumin (BSA)/ phosphate buffered saline solution (PBS) for 30 minutes and stained with a rabbit anti mouse Beta actin antibody (ABCAM) at 1µg/ml in 1%BSA/PBS, as a cell marker (and to identify glomerular regions of tissue for measurement) overnight at 4°C. For secondary detection a chicken anti rabbit Alexa Fluor 488 antibody at 1:200 was used for 40 minutes at RT (Molecular Probes, Thermofisher). Slides were quenched in Sudan Black as outlined above and mounted with DAPI prolong gold mounting media to detect DNA. NETs and extracellular MPO were detected as published previously (18). Briefly, Sections (3 µm) of formalin-fixed, paraffin-embedded tissue specimens were mounted on superfrost plus slides

(Menzel, Braunschweig, Germany), dewaxed, rehydrated, and pre-treated with antigen retrieval solution Tris-EDTA pH 9 (10mM TRIS, 1mM EDTA)in a pressure cooker for 10 min, blocked (30 min) in either 10% chicken sera in 5% bovine serum albumin/phosphate-buffered saline (immunofluorescence) and probed with antibodies against goat anti human MPO (detects Mouse MPO) rat anti mouse CD45 for the detection of extracellular MPO, and mouse anti human PAD4, rabbit anti human H3Cit, and goat anti human MPO in 1% bovine serum for the detection of NETs, diluted in albumin/phosphate-buffered saline for 16 h (4 °C). Secondary detection was with either Alexa Fluor 594-conjugated chicken anti goat IgG or Alexa Fluor 488-conjugated chicken anti-rabbit IgG, or donkey anti mouse 647 IgG (all, from Molecular Probes 1:200, 40 min, room temperature). To quench tissue auto fluorescence, slides were incubated with Sudan Black (Sigma-Aldrich St Louis, MO, 0.1% in 70% ethanol, 30 min), washed in phosphate-buffered saline, and cover slipped in DAPI prolong gold (Molecular Probes). Fluorescent images were acquired using a NIKON C1 confocal laser scanning head attached to Nikon Ti-E inverted microscope (Coherent Scientific, SA, Australia); 405, 488, and 561 nm 647nm lasers were used to specifically excite DAPI, Alexa 488, Alexa 594, and Alexa 647. Single plane 512 × 512 × 12 bit images were captured in a line-sequential manner (4 line averaging) using a 20 ×, 40 ×, or 60 × objective.

Assessment of ecDNA, extracellular MPO and DNase I

To measure the ecDNA in both human renal biopsies and murine kidneys, a published method using “analyse particle” in image J was used and circularity set to include nuclear staining, the nuclear stain was thresholded, marked and excluded from analysis using the watershed function in Image J, leaving only the extranuclear stain to be measured (NIH, Bethesda, MD)(41). The average integrated intensity/density was used and expressed in arbitrary units per glomerular cross section. Extracellular MPO was measured by a previously published method using a macro in Image J analysis software (NIH, Bethesda, MD)(30). Intracellular (leukocyte-associated) MPO

was defined being associated with CD45 (CD45+MPO+ cells). Extracellular MPO was measured as MPO+CD45 staining. The macro evaluated both the area and intensity and expressed the results as arbitrary units (AU).

Assessment of renal human and mouse DNase I

Histologic assessment of renal injury was performed on 3 mm thick, formalin-fixed, paraffin-embedded human renal biopsies from AAV patients and MCD patients, and murine models of anti MPO-GN and GN induced by passive ANCA. Sections were cleared in Histosol, rehydrated in graded alcohols and then blocked with 10% Horse serum in 5% BSA/PBS for 30 minutes at RT and incubated with a mouse anti human DNase I antibody (1/100, Santa Cruz) over night at 4 degrees. Sections were washed, and endogenous peroxidase blocked with 1% Hydrogen Peroxide (H202) in Methanol for 20 minutes, followed by blocking with avidin and biotin using a commercially available blocking kit per manufacturer's instructions (Vector Laboratories). Secondary antibody detection was performed with a horse anti mouse biotinylated antibody at 1/60 (Vector Laboratories) for 40 minutes at RT, and detected with an avidin biotin complex conjugated to HRP (ABC-HRP) for 40 minutes (Vector Laboratories), and detected with 3,3′-Diaminobenzidine (DAB brown, SIGMA), dehydrated, cleared in histosol and mounted in vector shield permanent mounting media. Five low powered (20x objective lens) fields of view of the tubulointerstitium were analyzed and graded 1-3 according to the amount of stain present within tubulointerstitial epithelial cells in the renal biopsies and 10 field of view were analyzed for mouse kidney tubulointerstitium.

Assessment of renal injury and leukocyte infiltration

Histologic assessment of renal injury was performed on 3 mm thick, formalin-fixed, paraffin-embedded, periodic acid-Schiff-stained kidney sections. A minimum of 30 consecutive glomeruli/mouse were examined and results expressed as percentage of segmental glomerular

necrosis per glomerular cross-section (gcs). Glomerular CD4+ T cells, macrophages, and neutrophils were assessed by an immunoperoxidase-staining technique described in the previous section, on 6-mm thick, periodate lysine paraformaldehyde (PLP) fixed, OCT frozen kidney sections. The primary antibodies used were GK1.5 for CD4+ T cells (anti-mouse CD4+;American Type Culture Collection, Manassas, VA), FA/11 for macrophages (anti-mouse CD68 from Dr. Gordon L. Koch, Cambridge, England), and RB6–8CS for neutrophils (anti- GR-1; DNAX, Palo Alto, CA). A minimum of 30 glomeruli were assessed and results expressed as cells/gcs (c/gcs).

Systemic Immune Responses to MPO

ELISA was used to detect circulating serum anti-MPO IgG titers using 100µl/well, 1µg/ml murine MPO and horseradish peroxidase conjugated sheep anti-mouse IgG (1:1000; Amersham Biosciences, Rydalmere, Australia). IFN-γ and IL-17A production was assessed by ELISPOT (BD Biosciences, Mouse IFN-γ ELISPOT kit and Mouse IL-17A ELISPOT kit) with draining LN cells seeded at $5x10^5$ cells/well restimulated with 10µg/ml of recombinant MPO for 18 hours. IFN-γ and IL-17A producing cells were enumerated with an automated ELISPOT reader system (TECAN). To assess MPO-specific dermal DTH, mice were challenged by intradermal injection of 10 mg murine MPO in 30 ml saline in the right hind footpad (the contralateral footpad received saline). DTH was quantified 24 hours later by measuring the difference between footpad thicknesses (Δmm) using a micrometer. For assessment of MPO specific cell cytokine production, lymphocytes were cultured for 16 hours (37°C, 5% CO2) 5x 10^5 cells/ml per well with or without MPO (10 µg/ml) in supplemented RPMI.

Flow cytometry and intracellular staining

DCs were identified as $CD11c^{hi}$ cells on isolated draining LN cells as measured by flow

cytometry. LN cells were stained for 30 minutes at 4˚C with the following directly conjugated antibodies: hamster anti-mouse CD11c PE (HL3), hamster anti-mouse CD11c PerCP/Cy5.5 (N418, BioLegend), rat anti-mouse CD40 FITC (3/32, BD Biosciences), rat anti-mouse MHC-II APC/Cy7 (M5/114.15.2, BioLegend), rat anti-mouse ICOS Ligand PE (HK5.3, Biolegend), mouse anti-mouse OX40L PE (8F4, Biolegend), hamster anti-mouse CD80 FITC (16-10A1, eBioscience), rat anti-mouse CD86 APC/Cy7 (GL-1, Biolegend). CD4 (GK1.5, BD), CD69 (H1.2F3, BD). For analysis of Treg response 5 x 10^5 LN cells were cultured for 72 hours with 10µg/ml MPO. CTV, as per manufacturer's instructions was added at 0 hours and cells stained using anti- (Foxp3FJK-16s, EBioscience) and Foxp3 fixperm kit (Ebioscience) Cells were analysed on the Beckman Coulter Navios platform and data analysed using FlowJo software (TreeStar, Palo Alto, CA).

NET and Zymosan phagocytosis Assays

For the *in vitro* NET assay and zymosan phagocytosis assay *n*=5 C57BL/6J male mice were injected with aged 4% thioglycolate intraperitoneally. Neutrophils 2x10^5 were plated out in 24 well plates for immunostaining. Neutrophils were pre-incubated with DNase I at varying concentrations from 0-4ug/ml DNase I for 30 minutes prior to adding PMA (40µg/ml, SIGMA) for 3 hours at 37 degrees Celsius induce NET formation in serum free RPMI (SIGMA). Cells were fixed in paraformaldehyde (2%) supplemented with periodate and lysine overnight at 4 degrees Celsius. Cells were washed, permeabilised, blocked in 10% Chicken Sera and then stained from markers of NETs, myeloperoxidase (MPO, AF3667, R&D Systems, Minneapolis, MN), Citrulinated histone 3 (Ab5103, Abcam), and peptidylarginine deiminase 4 (PAD4; AB128086, Abcam), and detected with secondary chicken ant rabbit AF488 (Thermofisher), chicken and mouse AF647 (Thermofisher), and Chicken anti goat AF594 (Thermofisher), mounted in DAPI ProLong Gold (Molecular Probes, Thermo Fisher Scientific), and NETs were visualized by confocal fluorescence microscopy with a Nikon Ti-

E inverted microscope (Nikon Instruments, Melville, NY). Then, 405-, 488-, 561-, and 647-nm lasers were used to specifically excite DAPI, Alexa Fluor 488, Alexa Fluor 594, and Alexa Fluor 647.

For the zymosan phagocytosis assays neutrophil procurement was conducted as above using 4% thioglycolate, and plated out at $5x10^5$ into a 96 well plate overnight at 37 degrees Celsius, neutrophils were treated with 0-4µg/ml DNase I 30 minutes prior to the addition of PMA at 40µg/ml for 3 hours. The zymosan phagocytosis assay was then performed using a standard kit (Abcam), visualized using the kit detection reagent and read at an absorbance plate reader at OD 405nm (Tecan).

Real-Time PCR for gene expression

Kidneys were stored at minus 80 degrees until time of RNA extraction. RNA extraction was performed via a standard protocol using trizol, a High capacity cDNA reverse Transcription Kit (Applied Biosystems, Foster City, CA) was used to generate cDNA. Taqman Universal PCR Master Mix and Tagman Gene expressions assays were performed as per manufactures instructions and normalised to the house keeping gene *18S* (Applied Biosystems, Gene specificities for (*CCL2, CXCL1, CXCL2, IFNγ, IL-1β, IL-6, TNFα* and *DNase I*) and read on the 7900HT Fast Real-Time PCR System (Applied Biosystems).

Statistical Analyses

Results are expressed as the mean ± SEM. Kruskal-Wallis one-way analysis of variance was used for comparisons between 3 groups, Mann–Whitney t-test was used for non-parametric data and paired t-test for comparison in ex vivo co-culture experiments. All data were analyzed with GraphPad Version 6 (GraphPad Prism; GraphPad Software Inc., San Diego, CA). Differences were considered to be statistically significant if $P<0.05$.

Results

EcDNA is deposited in the glomerular of patients with MPO-ANCA vasculitis

To semi-quantitate the extent of ecDNA accumulation in kidneys of MPO-ANCA GN patients presenting with acute GN, we analyzed tissues collected from a cohort (*n*=29) and compared them with control tissues collected from patients with minimal change disease (MCD, *n*=6). The MPO-ANCA GN patients presented with severe renal disease with an estimated glomerular filtration rate (eGFR) of 34.77±8 (mean ±SEM, ml/min/1.73^2) compared to the control group that showed an eGFR of 100.1±6 (mean ± SEM ml/min/1.73^2), all patients had a positive MPO-ANCA, and an average of 18 glomeruli per biopsy (see other patient clinical data in Supplementary Table 1).

Renal biopsies were analyzed using a methodology that detects ecDNA regardless of the type of cell death (i.e. apoptotic, necrotic or NETotic). Fragmented ecDNA outside the nucleus of cells was assessed by semi-quantitative analysis of positive staining and expressed in arbitrary units. There was significantly greater ecDNA deposition within the glomeruli of MPO-ANCA GN biopsies compared to control biopsies (Figures 1, A-C). It has been reported that patients with MPO-ANCA GN have lower levels of circulating DNase I (17), which may impair NETs digestion and removal of apoptotic bodies. A subset of the 29 renal biopsies used to measure ecDNA were labelled (*n*=6, due to scarcity of tissue) with DNase I antibody demonstrated that MPO-ANCA GN patients have less DNase I expression within the tubulointerstitium and glomeruli when compared to those from control MCD patients (*n*=6) (Figure 1D).

Enhanced deposition of ecDNA and reduced expression of DNase I in the kidneys of mice with anti-MPO GN is attenuated with exogenous DNase I administration

Using an established murine model of anti-MPO GN (38), we tested the hypothesis that disease is associated with increased levels of ecDNA deposition in murine kidneys. Mice

were immunized with MPO and GN was induced with anti-GBM immunoglobulin (Figure 2A, anti-GBM Ig). Glomerular injury in this model of active anti-MPO autoimmunity is mediated by cellular effectors and OVA-immunized mice serve as negative controls. Compared with control mice, anti-MPO GN mice exhibited higher levels of ecDNA deposition and significantly less DNase I expression (Figure 2B). Thus, this model shows the same pattern of injury with respect to ecDNA and decreased DNase I expression as observed in the human disease. (Figure 1A). To test whether the reductions in endogenous DNase I levels could be offset using exogenous DNase I to alleviate clinical endpoints of disease, anti-MPO GN mice were given twice daily injections of human DNase I for four days. This treatment significantly attenuated glomerular ecDNA deposition (Figures 2B-C) and restored renal expression of DNase I when compared to control animals (Figure 2D). As expected, endogenous DNase I levels were unaffected in OVA control mice, which also did not develop anti-MPO autoimmunity as seen by the absence of GN, low levels of ecDNA deposition, NET formation and MPO deposition (Figure 2 B-E, Supplementary Figures 1 and 2).

Exogenous DNase I treatment diminishes glomerular injury and glomerular NET formation in MPO-ANCA GN

Having demonstrated that DNase I cleared ecDNA and maintained homeostasis of endogenous renal DNase I, further endpoints were assessed to determine the effect of enzyme administration on other disease biomarkers. DNase I treated mice showed significantly reduced glomerular injury as seen by reductions in abnormal glomeruli (Figure 3A-B), fibrin deposition (Figure 3C-D) and glomerular DTH effector cell influx when compared to saline control mice that developed anti-MPO GN (Figure 3E-G). Albuminuria over 24 hours was reduced in the DNase I treated mice when compared to control mice but this did not reach statistical significance (P=0.06, Figure 3H). DNase I was administered to mice 16 days after establishment of autoimmunity and GN initiated with anti-GBM Ig. Despite only 4 days of

treatment, DNase I treated mice had a significant reduction in dermal DTH, measured by a 24-hour footpad MPO challenge compared with saline treated control group (Figure 3I). Assessment of the number of MPO-specific IFNγ and IL17A producing cells from lymph node draining sites of MPO immunization in the DNase I treated group demonstrated a significant reduction in both these cell populations (Figures 3J-K).

In vehicle-treated mice developing anti-MPO GN, NETs were found in 80% of glomeruli, while DNase I treatment significantly reduced the number of glomeruli with NETs to less than 10% (Figure 4A-B). The reduction in NETs was associated with significant reductions in extracellular MPO deposition (Figure 4C-D).

Exogenous DNase I attenuates the development of anti-MPO autoimmunity.

To assess the effect of exogenous DNase I on the development of MPO autoimmunity, DNase I or vehicle control was administered to C57BL/6 WT mice (*n*=10 each group) one day prior to the groups receiving subcutaneous immunization with recombinant murine MPO emulsified in FCA, followed by daily injections of saline or DNase I for a further ten days (Figure 5A). When compared to saline control mice, DNase I treated mice had a significant reduction in dermal DTH, as measured by a 24-hour footpad challenge with MPO (Figure 5B), but no significant difference in anti-MPO-ANCA titers were observed between groups (Figure 5C). *Ex vivo* stimulation of cells from the lymph nodes that drain immunization sites demonstrated that DNase I significantly reduced the numbers of IFN-γ secreting cells detected via ELISPOT (Figure 5D) whereas IL17A responses remained unchanged across groups (Figure 5E). Moreover, draining lymph node lymphocytes in this assay had a significant increase in $CD4^{+}Foxp3^{+}CTV^{-}$ cells (Figure 5F). Collectively, this data strongly indicates that DNase I inhibits the development of anti-MPO autoimmunity by both reducing the frequency of Th1 MPO-specific effector cells whilst increasing the frequency of MPO-specific T

regulatory cells.

Exogenous DNase I inhibits DC migration and activation in lymph nodes draining MPO immunization sites.

To test the hypothesis that DNase I modulates DC activation after MPO immunization, the effects of DNase I was examined at the time of antigen presentation. C57BL/6 mice received ivDNase I 24-hours before immunization with MPO in FCA and mice were culled 18 hours later (Figure G). Draining lymph nodes were removed and CD11c+ cells examined by FACs analysis for co-expression of activation markers. Eighteen hours after immunization with MPO, the mice treated with ivDNase I had a significant reduction in the proportion of CD11c +ve (Figure 5H). Also, DCs migrating to the draining lymph nodes showed a reduction in the expression of activation and co-stimulation markers CD80, CD86, CD40, OX40L, ICOS, and MHC class II (Figures 5, I-N). The ivDNase I treated group also had a significant reduction in the proportion of activated T cells (CD4+CD69+, Figure 5O). These findings are consistent with DNase I inhibition of DC activation and migration to draining nodes. They also support the view that DNA (in adjuvants or potentially from damaged cells) is a potent/essential component of successful induction of MPO autoimmunity and that DNase I may be used as a "biological" therapeutic to attenuate the development of anti-MPO autoimmunity.

DNase I attenuates establishment of disease in a second murine model of MPO-ANCA induced GN

The International Society of Nephrology recommend therapeutic drug testing is undertaken in multiple pre-clinical animal models (42) so therapeutic efficacy of DNase I shown in the 20-day T cell-mediated model of anti MPO-GN was also tested in a second model of anti-MPO GN, which isolates the effect of on MPO-ANCA induced glomerular injury. We utilized a well-characterized 6-day model of glomerular injury induced by passive transfer of LPS and

high-titer MPO-ANCA (43), which is triggered via infusion of anti-MPO Ig (raised in hyperimmunized MPO-/- mice). DNase I (or vehicle) was given 24 hours prior to disease induction and 12 hourly until the end of the experiment (Figure 6A). Renal ecDNA deposition was significantly less (Figure 6B-C, $p<0.05$) and DNase I expression was significantly greater in ivDNase I treated mice than in vehicle-treated mice developing passive ANCA GN ((Figure 6D-E, $p<0.05$). Glomerular NET formation (Figure 7A-B) and deposition of extracellular MPO (Figure 7C-D) were both significantly greater ($p<0.05$) in control vehicle-treated mice than in animals that received ivDNase I. Histological assessment of glomerular injury demonstrated ivDNase I treatment prevented the development of abnormal glomeruli (Figure 8A-B) and reduced the numbers of glomerular infiltrating polymorphonuclear leukocytes (Figure 8C-D), macrophages (Figure 8E-F) and CD4 T cells (Figure 8G-H). This was accompanied by a reduction in functional injury measured by albuminuria, although this did not reach significance (Figures 8I), as was also shown in the 20-day model. Analysis of kidney mRNA for common inflammatory markers demonstrated significant diminution of chemokines that control macrophage recruitment (CCL2, Figure 9A) neutrophil recruitment (CXCL1 and CXCL2, Figure 9B-C) and markers of inflammation including IFNγ, IL-1B, IL-6 and TNFα (Fig 9D-G). Analysis of mRNA for DNase I showed that non-treated mice had significantly more DNase I than the iv DNase I treated group indicating increased production of DNase I in an effort to clear the burden of ecDNA deposited in the kidney (Figure 9H). Collectively, these data in two models of anti-MPO autoimmune GN indicate that ecDNA deposition can be cleared by exogenous DNase I and that this breaks the vicious cycle of inflammation that propagates glomerular injury.

Adeno-associated viral vector delivery of DNase I has enhanced therapeutic efficacy over ivDNase I to reduce inflammation in MPO-ANCA GN

The ivDNase I treatment of the MPO-ANCA required twice daily doses to compensate for

short serum half-life of the enzyme. We investigated whether delivery of DNase I could be facilitated using adeno-associated virus vector to systemically deliver recombinant DNase I (Figure 10A). In our previous study, we have shown that within 3 days of vector injection the liver provides a continuous super-physiological supply of DNase I in the circulatory system that stably persists beyond the 6-month time-frame of the study (40) . Using our 20-day ANCA-MPO model, we gave a single dose of vector encoding either DNase I (vDNase I) or GFP (vGFP, Figure 10A) on day 10 after the establishment of autoimmunity to MPO (Figure 10B). This resulted in a ~200-fold increase in DNase I activity compared to either ivDNase I delivered twice daily or vGFP control treated animals (Figure 10C). vDNase I significantly reduced DTH similarly to ivDNase I (Figure 10D). Interestingly, vDNase I was able to significantly reduce the generation of MPO-ANCA whereas ivDNase I had no effect on ANCA levels (Figure 10E). vDNase I significantly reduced the number of both IFNγ and IL17a MPO specific effector cells in the draining lymph nodes (Figure 10F-G, similar to effects seen with intravenous DNase I administration in the previous sections (Figure 9E-F). Importantly, vDNase I also significantly reduced 24-hour albuminuria; a marked improvement over ivDNase I administration (Figure 11A). Further evidence for prevention of glomerular injury by vDNase I was seen with reductions in both segmental necrosis (Figure 11B) and recruitment of glomerular neutrophils, macrophages and CD4 T cells (Figure 11C-E). To further investigate the role of vDNase I in clearing ecDNA we investigated Caspase 3 and RIPK3 glomerular protein expression as markers of apoptosis and necroptotic cell death. Vector delivery of DNase I reduced expression of these proteins in comparison to the GFP-control vector group (Figure 11F). Collectively, these data show that gene therapy overcomes the issue of short half-life of DNase I to provide a superior treatment option for anti-MPO GN.

Exogenous DNase I concentrations required to inhibit NETs has no effect on neutrophil

phagocytosis

Administration of AAV-DNase I can produces more than six months of supraphysiological amounts of DNase I (40). A concern of having a continuous supply of DNase I is that ecDNA released via infectious agents, such as CpG from bacteria, may fail to trigger pattern recognition receptors and associated pro-inflammatory cascades required to eliminate pathogens. To investigate whether using DNase I as a potential therapeutic could compromise neutrophil phagocytosis, and therefore impede host protection, we conducted zymosan phagocytosis assays in the presence of DNase I. Thioglycolate elicited mouse peritoneal neutrophils were incubated with zymosan particles and varying concentrations of recombinant human DNase I (0-4µg/mL). No significant differences were detected between phagocytosis controls and neutrophils incubated with DNase I (Figure 11G) indicating that DNase I has no effect on neutrophil phagocytosis. The lowest concentration of DNase I was then used to inhibit NETosis in parallel experiments 1µg/ml (Figure 11H) which completely abrogated NET formation. Together, these *in vitro* results with the *in vivo* animal work suggest that DNase I can dampen inflammation caused by NETs whilst still permitting neutrophil phagocytosis from healthy neutrophils.

Discussion

It is widely accepted that NETs are a major driver of inflammation in MPO-ANCA GN through deposition of MPO, the autoantigen in the disease (17, 20, 29, 30). What is unclear is the contribution of ecDNA in perpetuating inflammation in MPO-ANCA GN. The current study strongly supports a role for ecDNA acting as a pro-inflammatory DAMP mediating injury and autoimmunity in MPO-ANCA GN. We show that ecDNA is a major feature in MPO-ANCA GN patient biopsies and that this is accompanied with a significant diminution of kidney DNase I expression. These observations were mirrored in two animal models of anti-MPO GN that show similar pathophysiology to human disease. We have also shown, for the first time, that administration of exogenous DNase I in experimental anti-MPO GN significantly diminished NETs, MPO and ecDNA deposition and preserved kidney DNase I expression levels. Moreover, this therapeutic effect was significantly enhanced when DNase I was delivered via gene transfer after one dose of an adeno- associated viral vector.

Our first aim in this study was to assess kidney biopsies from patients with autoimmune MPO-ANCA-GN with the hypothesis that release of ecDNA in renal disease disrupts DNase I homeostasis and capacity to clear ecDNA. After confirming significant ecDNA deposition in MPO-ANCA GN biopsies, the hypothesis was supported with the demonstration of significant diminution in the expression levels of renal DNase I when compared to control patients (Minimal Change Disease). This indicated that DNA may potentially play a significant injurious role in this disease.

NETs are integral to the pathophysiology of ANCA vasculitis and have been shown to be induced by MPO-ANCA/PR3-ANCA and are closely associated with the deposition of extracellular MPO within MPO-ANCA GN patient biopsies (17, 30, 44). MPO bound to ecDNA has greater biological activity and is shielded from endogenous inhibitors such as ceruloplasmin

(31). Together, this evidence indicates NETs are both a major driver of inflammation and source of autoantigens (17, 30, 44, 45). The capacity of exogenous DNase I to clear not only NET deposited injurious ecDNA but also DNA deposited from all forms of cell death reported in anti-MPO GN (necroptosis, apoptosis and necrosis) was tested in a 20-day murine model of actively induced autoimmune anti-MPO GN, which shows many of the hallmarks of human disease (20, 30, 46). MPO-ANCA GN can be characterized as both a type II antibody mediated disease (due to production of ANCA) and a type IV cell-mediated hypersensitivity (due to the Th1 cell mediated aspect of the disease) as per Gell and Coombs classification(47). We show that deposited extracellular MPO can be recognized by MPO-specific $CD4^+$ T cells that in turn initiate cell-mediated glomerular injury characterized by DTH effectors, including the glomerular recruitment of M1 macrophages and the deposition of fibrin, features of GN that is prominent in human and murine anti-MPO GN (48). Additional notable features of the model include generation of MPO-ANCA, patterns of glomerular injury and neutrophil infiltration (focal and segmental necrosis and leukocyte infiltration) and production of albuminuria/proteinuria (33-36). Administration of DNase I to mice with established anti-MPO GN was able to significantly reduce ecDNA, glomerular NET formation and MPO deposition. DNase I treatment also significantly attenuated MPO-specific dermal DTH and the frequency of kidney infiltration of CD4 T cells, macrophages and neutrophils indicative of DNase I inhibiting type IV cell mediated disease. Importantly, exogenous DNase I treatment also preserved DNase I expression levels in the kidney, which is important as depletion of DNase I expression in the organ would render it even more vulnerable to pathological assault induced by uncleared NETs and DNA.

Having established that DNase I is therapeutic even after establishment of MPO autoimmunity in the 20-day cell mediated model of anti MPO GN, we next dissected mechanisms by which DNase I reduces systemic autoimmune responses to MPO. While the mechanisms of DNase I clearance of ecDNA are well understood (28, 49, 50), the mechanisms by which this ecDNA

clearance attenuates anti-MPO autoimmunity and GN is unclear. To investigate this phenomenon, we utilized a 10-day model free of complicating GN to dissect out the role of DNase I in preventing systemic autoimmunity to MPO. We revealed that continued daily treatment using exogenous DNase I after animal immunization against MPO using FCA resulted in significant reductions in MPO-specific IFNγ producing cells as well as MPO-triggered dermal responses to DTH responses. However exogenous DNase I treatment failed to reduce MPO-ANCA levels. These results confirm a role for DNA in the induction of anti-MPO cellular autoimmunity. The source of this DNA comes from both the accompanying adjuvant, known to contain significant amounts of DNA, and from endogenous neutrophils attracted to sites of MPO immunization whereby they release NETs and DNA (51). Further supporting evidence for a role for DNA activation in MPO-ANCA GN comes from the capacity for DNA subcomponents (e.g. CpG, bacterial DNA components) alone to provide sufficient adjuvant support to allow MPO immunization to induce anti-MPO autoimmunity and GN (52, 53). Furthermore, in the 18-hour model, to dissect out the role DNase I may be playing at the time of antigen presentation, our studies show that DNase I treatment prior to MPO immunization significantly reduces the frequency of DCs in lymph nodes that drain immunization sites and that the DCs that are present show reductions in DC activation markers, including surface costimulatory molecules essential for driving naïve anti-MPO specific CD4 T cell activation and proliferation. DNase I inhibition of DC activation and lymph node migration supports the view that DNA (in adjuvants or recruited neutrophils) is a potent inducer of MPO autoimmunity and, for the first time, that DNase I may be used as a biological therapeutic to attenuate the development and/or perpetuation of anti-MPO autoimmunity.

DNA has been shown to provide a danger signal to both macrophages and DCs, which induces them to increase their expression of MHC class II expression and co-stimulatory molecules CD40 and CD80/86 (50, 51, 54). The mechanism of DNA activation involves selective DC uptake of the

autoantigen MPO by the scavenger receptor DEC-205 followed by binding to the DNA cytosolic receptor TLR9 (53, 55). Therefore, it is likely that DNase I acts by reducing local and/or systemic ecDNA levels thereby circumventing activation of DC and down-stream lymphoproliferative responses. MPO-pulsed DCs stimulated with TLR9 ligand CpG (a component of DNA) stimulates Th1 responses, MPO autoimmunity and promotes kidney injury in experimental anti-MPO GN (53). In contrast, mice receiving TLR9-/- DCs are protected from injury. Given the major ligand of TLR9 is DNA, this provides further supporting evidence that DNA is inflammatory and gives impetus to therapeutically target ecDNA (53). Furthermore, the observation that mice deficient in DNase I or DNase II develop autoimmunity spontaneously including glomerulonephritis provides additional support for a homeostatic/protective role for DNase I or DNase II (27, 56). Reinforcing the potential of DNase I treatment for acute renal injury are recent studies showing that exogenous DNase I is protective in a rat model of ischemia/reperfusion-induced acute kidney injury and also reduces necroptosis in murine ANCA vasculitis (20, 49) .

Having established the kinetics and consequence of early cell-mediated responses in the models, we then turned our attention to understanding the role of MPO-ANCA as this is highly relevant to human disease. ANCA binds to neutrophils inducing their infiltration into glomerular capillaries where they degranulate, produce ROS, undergo NETosis, deposit MPO extracellularly and initiate GN. To test the robustness of our findings in the cell-mediated 20-day model of anti MPO-GN we used a second model of vasculitis. We administered DNase I before administering LPS and passively transferring anti-MPO antibodies (MPO-ANCA) in a 6-day model and showed that this inhibited ANCA-mediated injury by reducing the amount of ecDNA able to activate innate immune inflammatory injury through DAMP pathways.

DNase I treatment of *in vitro* neutrophils has shown that DNase I is associated with a decrease in ROS levels and does not directly inhibit MPO, but degrades the extra-cellular matrix of MPO-

associated DNA, which decreases the biological activity of the MPO (57). These modulating effects on neutrophils in the circulation are likely to account for the significant reduction of ANCA-induced neutrophil accumulation in glomeruli. Exogenous DNase I abrogates NET formation, ecDNA deposition and significantly reduces glomerular neutrophil accumulation resulting in significant reductions in pathological injury (assessed by focal segmental necrosis). In the passive ANCA model of glomerular injury, T cell autoimmunity is absent therefore it can be used to directly assess the effects of DNase I on ANCA-mediated injury. However, both these models are of insufficient duration to effectively assess the effects of DNase I over longer-term development of ANCA.

It was of great interest in the current study to find that viral vector delivery in the 20-day model was able to reduce the titers of ANCA, whereas twice daily exogenous DNase I administration did not achieve this outcome. The sustained and supraphysiological levels of DNase I achieved via vector delivery also diminished kidney injury (segmental necrosis and albuminuria). This is likely to have occurred through reductions in DAMP DNA that prevent DC activation of CD4 T helper cells, which inhibits B cell activation and subsequent MPO-ANCA production by plasma cells. This finding might also account for the ineffectiveness of exogenous DNase I in an animal model of IgA nephropathy at reducing IgA and IgE levels (58). As NETs are also a prominent pathophysiological feature, correlate with disease severity and depleted circulatory DNase I in patients with this disease, it would be of great interest to see if vector delivery of DNase I has therapeutic benefit in IgA vasculitis too (59).

The human protein atlas shows that the kidney has one of the highest mRNA expression levels of DNase I compared to other organs in the body, but controversially the atlas shows that DNase I protein is not detected in the kidney (60, 61). This is also at odds with our results that show strong staining for DNase I in kidney tissue from patients with minimal change disease and that enzyme expression is notably depleted in patients with MPO-ANCA GN. Previous studies in

Lupus and membranous nephropathy have also demonstrated DNase I expression both in human and mouse studies (28, 62, 63). In particular, MPO-ANCA GN patients compared to lupus nephritis patients have enhanced loss of DNase I protein within the kidney. This was also observed in our models of anti-MPO GN where the ova immunised mice (mice without autoimmunity to MPO or GN) had significantly more DNase I protein expression than untreated mice and exogenous DNase I partially restored this level in the kidney. Collectively, these results indicate the human protein atlas may require reinvestigation for DNase I protein.

DNase I has been shown to be critical in preventing chronic neutrophilia. *DNase 1-/- DNase 1L3 -/-* mice have intravascular occlusions, with NETs entrapping platelet and ethryocytes (64). DNase 1L3 is expressed in immune cells, whereas DNase I is secreted by non-hematopoietic tissue. Restoring either of the DNase enzymes in double knock-out mice prevented neutrophil accumulation NET formation and premature death. This adds weight to the argument that constant systemic release of DNase I is required to clear neutrophil derived DNA.

There has been considerable interest for many decades in clinically translating recombinant DNase I in multiple different disease contexts. In the pre- antibiotic era, the enzyme was used topically to clear and sterilize infected wounds and relieve meningitis (65). Currently, it is administered in nebulized form to the airways of cystic fibrosis patients to degrade nuclear material released from dead neutrophils, thereby reducing viscosity of respiratory secretions (66). Intravenous DNase I has also been used in clinical trials of SLE where it was shown to be safe and well-tolerated, albeit ineffective in disease control possibly because of its relatively short half-life in serum (<5 hours)(67). Our study has shown gene delivery provides a solution to this issue and creates an option that is therapeutically superior to intravenous enzyme delivery. Adeno-associated virus vectors have a strong safety profile and permit long-term transgene expression in post-mitotic cells (>10 years in the liver) making them ideally suited to treat chronic and remitting diseases such as MPO-ANCA GN, which requires life-long and ongoing

treatment (68-70). Additionally, use of a vector that targets hepatocytes to release DNase I systemically circumvents the limitations of vector entering the kidney through the specialized glomerular basement membranes which have a filtering exclusion limit of 50kDa (71). Furthermore, as MPO-ANCA GN patients have significantly damaged kidney's in particular endothelial cells and podocytes, tissue pathology may be a barrier to successful gene transfer. Systemic release of DNase I via the liver hepatocytes will not only target ecDNA in the kidney but will have further therapeutic benefit by also digesting DNA being released from cell death within the circulation. Further development of the technology to pharmacologically regulate transgene expression would offer the remarkable prospect of switching therapy "on and off" to regulate vector dosing of DNase I, thus allowing for periods of active disease versus remission (72). The therapeutic efficacy of vector-delivered DNase I in a murine model that emulates human MPO-ANCA GN supports the possibility that this gene therapy could be a powerful approach in treating clinical disease for a patient cohort with limited treatment options.

Acknowledgments

We acknowledge funding support from the National Health and Medical Research Council of Australia (ID 2020579) and the Rebecca L Cooper Foundation (PG2019449); Monash Micro Imaging for the provision of the Nikon, Confocal Microscope, Monash Health Translational Precinct Flowcore for FACS, the Monash Health and Translational Genomics Platform for RT-PCR machine access and the Australian Government for providing a Research Training Program Scholarship.

REFERENCES

1. Flossmann O, Berden A, de Groot K, Hagen C, Harper L, Heijl C, et al. Long-term patient survival in ANCA-associated vasculitis. *Ann Rheum Dis.* 2011;70(3):488-94.
2. Kitching AR, Anders H-J, Basu N, Brouwer E, Gordon J, Jayne DR, et al. ANCA-associated vasculitis. *Nature Reviews Disease Primers.* 2020;6(1):71.
3. Falk RJ. ANCA-associated renal disease. *Kidney international.* 1990;38(5):998-1010.
4. Falk RJ, Hogan S, Carey TS, and Jennette JC. Clinical course of anti-neutrophil cytoplasmic autoantibody-associated glomerulonephritis and systemic vasculitis. The Glomerular Disease Collaborative Network. *Annals of internal medicine.* 1990;113(9):656-63.
5. Falk RJ, Hogan SL, Wilkman AS, Terrell RS, Lauritzen S, Charles LA, et al. Myeloperoxidase specific anti-neutrophil cytoplasmic autoantibodies (MPO-ANCA). *The Netherlands journal of medicine.* 1990;36(3-4):121-5.
6. Falk RJ, Terrell RS, Charles LA, and Jennette JC. Anti-neutrophil cytoplasmic autoantibodies induce neutrophils to degranulate and produce oxygen radicals in vitro. *Proceedings of the National Academy of Sciences of the United States of America.* 1990;87(11):4115-9.
7. Galluzzi L, Kepp O, Chan FK, and Kroemer G. Necroptosis: Mechanisms and Relevance to Disease. *Annu Rev Pathol.* 2017;12:103-30.
8. Brinkmann V, Reichard U, Goosmann C, Fauler B, Uhlemann Y, Weiss DS, et al. Neutrophil extracellular traps kill bacteria. *Science.* 2004;303(5663):1532-5.
9. Desai J, Mulay SR, Nakazawa D, and Anders HJ. Matters of life and death. How neutrophils die or survive along NET release and is "NETosis" = necroptosis? *Cell Mol Life Sci.* 2016;73(11-12):2211-9.
10. Fuchs TA, Abed U, Goosmann C, Hurwitz R, Schulze I, Wahn V, et al. Novel cell death program leads to neutrophil extracellular traps. *J Cell Biol.* 2007;176(2):231-41.
11. Neeli I, Khan SN, and Radic M. Histone deimination as a response to inflammatory stimuli in neutrophils. *J Immunol.* 2008;180(3):1895-902.
12. Jorgensen I, Rayamajhi M, and Miao EA. Programmed cell death as a defence against infection. *Nat Rev Immunol.* 2017;17(3):151-64.
13. O'Sullivan KM, and Holdsworth SR. Neutrophil Extracellular Traps: A Potential Therapeutic Target in MPO-ANCA Associated Vasculitis? *Front Immunol.* 2021;12:635188.
14. Wigerblad G, and Kaplan MJ. Neutrophil extracellular traps in systemic autoimmune and autoinflammatory diseases. *Nature Reviews Immunology.* 2023;23(5):274-88.
15. Huang SU, and O'Sullivan KM. The Expanding Role of Extracellular Traps in Inflammation and Autoimmunity: The New Players in Casting Dark Webs. *Int J Mol Sci.* 2022;23(7).
16. Dhanwani R, Takahashi M, and Sharma S. Cytosolic sensing of immuno-stimulatory DNA, the enemy within. *Curr Opin Immunol.* 2018;50:82-7.
17. Kessenbrock K, Krumbholz M, Schonermarck U, Back W, Gross WL, Werb Z, et al. Netting neutrophils in autoimmune small-vessel vasculitis. *Nat Med.* 2009;15(6):623-5.
18. Lande R, Ganguly D, Facchinetti V, Frasca L, Conrad C, Gregorio J, et al. Neutrophils activate plasmacytoid dendritic cells by releasing self-DNA-peptide complexes in systemic lupus erythematosus. *Sci Transl Med.* 2011;3(73):73ra19.
19. Lande R, Gregorio J, Facchinetti V, Chatterjee B, Wang YH, Homey B, et al. Plasmacytoid dendritic cells sense self-DNA coupled with antimicrobial peptide. *Nature.* 2007;449(7162):564-9.
20. Schreiber A, Rousselle A, Becker JU, von Massenhausen A, Linkermann A, and Kettritz R. Necroptosis controls NET generation and mediates complement activation, endothelial damage, and autoimmune vasculitis. *Proceedings of the National Academy of Sciences of the United States of America.* 2017;114(45):E9618-E25.
21. Yoneyama M, and Fujita T. Cytoplasmic double-stranded DNA sensor. *Nature Immunology.* 2007;8:907.
22. Abe T, and Barber GN. Cytosolic-DNA-mediated, STING-dependent proinflammatory gene induction necessitates canonical NF-kappaB activation through TBK1. *J Virol.* 2014;88(10):5328-41.
23. Dombrowski Y, Peric M, Koglin S, Kammerbauer C, Goss C, Anz D, et al. Cytosolic DNA triggers

inflammasome activation in keratinocytes in psoriatic lesions. *Sci Transl Med.* 2011;3(82):82ra38.
24. Santa P, Garreau A, Serpas L, Ferriere A, Blanco P, Soni C, et al. The Role of Nucleases and Nucleic Acid Editing Enzymes in the Regulation of Self-Nucleic Acid Sensing. *Front Immunol.* 2021;12:629922.
25. Basnakian AG, Singh AB, and Shah SV. Identification and expression of deoxyribonuclease (DNase) I alternative transcripts in the rat. *Gene.* 2002;289(1):87-96.
26. Ershova E, Sergeeva V, Klimenko M, Avetisova K, Klimenko P, Kostyuk E, et al. Circulating cell-free DNA concentration and DNase I activity of peripheral blood plasma change in case of pregnancy with intrauterine growth restriction compared to normal pregnancy. *Biomed Rep.* 2017;7(4):319-24.
27. Napirei M, Karsunky H, Zevnik B, Stephan H, Mannherz HG, and Moroy T. Features of systemic lupus erythematosus in Dnase1-deficient mice. *Nat Genet.* 2000;25(2):177-81.
28. Zykova SN, Tveita AA, and Rekvig OP. Renal Dnase1 enzyme activity and protein expression is selectively shut down in murine and human membranoproliferative lupus nephritis. *PLoS One.* 2010;5(8).
29. Nakazawa D, Shida H, Tomaru U, Yoshida M, Nishio S, Atsumi T, et al. Enhanced formation and disordered regulation of NETs in myeloperoxidase-ANCA-associated microscopic polyangiitis. *J Am Soc Nephrol.* 2014;25(5):990-7.
30. O'Sullivan KM, Lo CY, Summers SA, Elgass KD, McMillan PJ, Longano A, et al. Renal participation of myeloperoxidase in antineutrophil cytoplasmic antibody (ANCA)-associated glomerulonephritis. *Kidney international.* 2015;88(5):1030-46.
31. Parker H, Albrett AM, Kettle AJ, and Winterbourn CC. Myeloperoxidase associated with neutrophil extracellular traps is active and mediates bacterial killing in the presence of hydrogen peroxide. *J Leukoc Biol.* 2012;91(3):369-76.
32. Takai T, Ono M, Hikida M, Ohmori H, and Ravetch JV. Augmented humoral and anaphylactic responses in Fc gamma RII-deficient mice. *Nature.* 1996;379(6563):346-9.
33. Gan P-Y, Chan A, Ooi JD, Dick J, Nagai K, O'Sullivan KM, et al. Biologicals targeting T helper cell subset differentiating cytokines are effective in the treatment of murine anti-myeloperoxidase glomerulonephritis. *Kidney international.* 2019;96(5):1121-33.
34. Gan P-Y, Dick J, O'Sullivan KM, Oudin V, Cao Le A, Koo Yuk Cheong D, et al. Anti-CD20 mAb-Induced B Cell Apoptosis Generates T Cell Regulation of Experimental Myeloperoxidase ANCA-Associated Vasculitis. *Journal of the American Society of Nephrology.* 2021;32(5).
35. Gan P-Y, Fujita T, Ooi JD, Alikhan MA, Dick J, Shim R, et al. Pathogenic Role for γδ T Cells in Autoimmune Anti-Myeloperoxidase Glomerulonephritis. *The Journal of Immunology.* 2017;199(9):3042-50.
36. Gan P-Y, Godfrey AS, Ooi JD, O'Sullivan K-M, Oudin V, Kitching AR, et al. Apoptotic Cell–Induced, Antigen-Specific Immunoregulation to Treat Experimental Antimyeloperoxidase GN. *Journal of the American Society of Nephrology.* 2019;30(8).
37. Apostolopoulos J, Ooi JD, Odobasic D, Holdsworth SR, and Kitching AR. The isolation and purification of biologically active recombinant and native autoantigens for the study of autoimmune disease. *Journal of immunological methods.* 2006;308(1-2):167-78.
38. Summers SA, van der Veen BS, O'Sullivan KM, Gan PY, Ooi JD, Heeringa P, et al. Intrinsic renal cell and leukocyte-derived TLR4 aggravate experimental anti-MPO glomerulonephritis. *Kidney international.* 2010;78(12):1263-74.
39. Ooi JD, Gan P-Y, Chen T, Eggenhuizen PJ, Chang J, Alikhan MA, et al. FcγRIIB regulates T-cell autoreactivity, ANCA production, and neutrophil activation to suppress anti-myeloperoxidase glomerulonephritis. *Kidney international.* 2014;86(6):1140-9.
40. Ahmad A, Mandwie M, O'Sullivan KM, Smyth C, York J, Doyle H, et al. Conversion of the Liver into a Biofactory for DNaseI Using Adeno-Associated Virus Vector Gene Transfer Reduces Neutrophil Extracellular Traps in a Model of Systemic Lupus Erythematosus. *Hum Gene Ther.* 2022;33(9-10):560-71.
41. O'Sullivan KM, Creed S, Gan PY, and Holdsworth SR. Supervised Machine Learning for Semi-Quantification of Extracellular DNA in Glomerulonephritis. *J Vis Exp.* 2020(160).
42. Nangaku M, Kitching AR, Boor P, Fornoni A, Floege J, Coates PT, et al. International Society of

Nephrology first consensus guidance for preclinical animal studies in translational nephrology. *Kidney international.* 2023;104(1):36-45.
43. Xiao H, Heeringa P, Hu P, Liu Z, Zhao M, Aratani Y, et al. Antineutrophil cytoplasmic autoantibodies specific for myeloperoxidase cause glomerulonephritis and vasculitis in mice. *The Journal of clinical investigation.* 2002;110(7):955-63.
44. Kraaij T, Kamerling SWA, van Dam LS, Bakker JA, Bajema IM, Page T, et al. Excessive neutrophil extracellular trap formation in ANCA-associated vasculitis is independent of ANCA. *Kidney international.* 2018;94(1):139-49.
45. van Dam LS, Kraaij T, Kamerling SWA, Bakker JA, Scherer UH, Rabelink TJ, et al. Intrinsically Distinct Role of Neutrophil Extracellular Trap Formation in Antineutrophil Cytoplasmic Antibody-Associated Vasculitis Compared to Systemic Lupus Erythematosus. *Arthritis Rheumatol.* 2019;71(12):2047-58.
46. Harper L, Cockwell P, Adu D, and Savage CO. Neutrophil priming and apoptosis in anti-neutrophil cytoplasmic autoantibody-associated vasculitis. *Kidney international.* 2001;59(5):1729-38.
47. Dispenza MC. Classification of hypersensitivity reactions. *Allergy Asthma Proc.* 2019;40(6):470-3.
48. Cunningham MA, Huang XR, Dowling JP, Tipping PG, and Holdsworth SR. Prominence of cell-mediated immunity effectors in "pauci-immune" glomerulonephritis. *J Am Soc Nephrol.* 1999;10(3):499-506.
49. Peer V, Abu Hamad R, Berman S, and Efrati S. Renoprotective Effects of DNAse-I Treatment in a Rat Model of Ischemia/Reperfusion-Induced Acute Kidney Injury. *Am J Nephrol.* 2016;43(3):195-205.
50. Suzuki K, Mori A, Ishii KJ, Saito J, Singer DS, Klinman DM, et al. Activation of target-tissue immune-recognition molecules by double-stranded polynucleotides. *Proceedings of the National Academy of Sciences of the United States of America.* 1999;96(5):2285-90.
51. Stephen J, Scales HE, Benson RA, Erben D, Garside P, and Brewer JM. Neutrophil swarming and extracellular trap formation play a significant role in Alum adjuvant activity. *NPJ Vaccines.* 2017;2:1.
52. Summers SA, Steinmetz OM, Gan PY, Ooi JD, Odobasic D, Kitching AR, et al. Toll-like receptor 2 induces Th17 myeloperoxidase autoimmunity while Toll-like receptor 9 drives Th1 autoimmunity in murine vasculitis. *Arthritis Rheum.* 2011;63(4):1124-35.
53. Ford SL, O'Sullivan KM, Kitching AR, Holdsworth SR, Gan PY, and Summers SA. Toll-like Receptor 9 Induced Dendritic Cell Activation Promotes Anti-Myeloperoxidase Autoimmunity and Glomerulonephritis. *Int J Mol Sci.* 2023;24(2).
54. Ishii KJ, Suzuki K, Coban C, Takeshita F, Itoh Y, Matoba H, et al. Genomic DNA released by dying cells induces the maturation of APCs. *J Immunol.* 2001;167(5):2602-7.
55. Odobasic D, Kitching AR, Yang Y, O'Sullivan KM, Muljadi RC, Edgtton KL, et al. Neutrophil myeloperoxidase regulates T-cell-driven tissue inflammation in mice by inhibiting dendritic cell function. *Blood.* 2013;121(20):4195-204.
56. Yoshida H, Okabe Y, Kawane K, Fukuyama H, and Nagata S. Lethal anemia caused by interferon-beta produced in mouse embryos carrying undigested DNA. *Nat Immunol.* 2005;6(1):49-56.
57. Munafo DB, Johnson JL, Brzezinska AA, Ellis BA, Wood MR, and Catz SD. DNase I inhibits a late phase of reactive oxygen species production in neutrophils. *Journal of innate immunity.* 2009;1(6):527-42.
58. Chen XQ, Tu L, Tang Q, Zou JS, Yun X, and Qin YH. DNase I targeted degradation of neutrophil extracellular traps to reduce the damage on IgAV rat. *PLoS One.* 2023;18(10):e0291592.
59. Chen X-Q, Tu L, Zou J-S, Zhu S-Q, Zhao Y-J, and Qin Y-H. The Involvement of Neutrophil Extracellular Traps in Disease Activity Associated With IgA Vasculitis. *Frontiers in Immunology.* 2021;12.
60. Ponten F, Jirstrom K, and Uhlen M. The Human Protein Atlas--a tool for pathology. *J Pathol.* 2008;216(4):387-93.
61. Atlas THP. The Human Protein Atlas. Human Protein Atlas proteinatlas.org. Accessed 19/03/2024.
62. Pedersen HL, Horvei KD, Thiyagarajan D, Norby GE, Seredkina N, Moroni G, et al. Lupus nephritis: low urinary DNase I levels reflect loss of renal DNase I and may be utilized as a biomarker of disease progression. *J Pathol Clin Res.* 2018;4(3):193-203.

63. Thiyagarajan D, Rekvig OP, and Seredkina N. TNFα Amplifies DNaseI Expression in Renal Tubular Cells while IL-1β Promotes Nuclear DNaseI Translocation in an Endonuclease-Inactive Form. *PLoS One.* 2015;10(6):e0129485.
64. Jiménez-Alcázar M, Rangaswamy C, Panda R, Bitterling J, Simsek YJ, Long AT, et al. Host DNases prevent vascular occlusion by neutrophil extracellular traps. *Science.* 2017;358(6367):1202-6.
65. Miller JM, and Ablondi F. A comparison of streptokinase and streptodornase with urea in the treatment of surgical infections. *Lancet.* 1953;265(6785):568-70.
66. Shak S, Capon DJ, Hellmiss R, Marsters SA, and Baker CL. Recombinant human DNase I reduces the viscosity of cystic fibrosis sputum. *Proceedings of the National Academy of Sciences of the United States of America.* 1990;87(23):9188-92.
67. Davis JC, Jr., Manzi S, Yarboro C, Rairie J, McInnes I, Averthelyi D, et al. Recombinant human Dnase I (rhDNase) in patients with lupus nephritis. *Lupus.* 1999;8(1):68-76.
68. Sobh M, Lagali PS, Ghiasi M, Montroy J, Dollin M, Hurley B, et al. Safety and Efficacy of Adeno-Associated Viral Gene Therapy in Patients With Retinal Degeneration: A Systematic Review and Meta-Analysis. *Transl Vis Sci Technol.* 2023;12(11):24.
69. Naso MF, Tomkowicz B, Perry WL, 3rd, and Strohl WR. Adeno-Associated Virus (AAV) as a Vector for Gene Therapy. *BioDrugs.* 2017;31(4):317-34.
70. Chuecos MA, and Lagor WR. Liver directed adeno-associated viral vectors to treat metabolic disease. *J Inherit Metab Dis.* 2024;47(1):22-40.
71. Rubin JD, Nguyen TV, Allen KL, Ayasoufi K, and Barry MA. Comparison of Gene Delivery to the Kidney by Adenovirus, Adeno-Associated Virus, and Lentiviral Vectors After Intravenous and Direct Kidney Injections. *Hum Gene Ther.* 2019;30(12):1559-71.
72. Monteys AM, Hundley AA, Ranum PT, Tecedor L, Muehlmatt A, Lim E, et al. Regulated control of gene therapies by drug-induced splicing. *Nature.* 2021;596(7871):291-5.

Figure Legends:

Figure 1. Enhanced extracellular DNA deposition and reduced DNase I expression in kidney biopsies from patients with MPO-ANCA GN. (A) Renal biopsies from ANCA-vasculitis patients were stained for double-stranded DNA (dsDNA) (red) and counterstained with β-actin (green) to aid in identification of glomeruli and cells. Biopsies from patients with minimal change disease (MCD) (with minimal glomerular injury) served as controls. Inset box shows higher power field of view with minimal ecDNA. (B) Patients with MPO-ANCA vasculitis show extensive peri-glomerular and glomerular ecDNA. (C) Semi-quantitation of extracellular dsDNA deposition in ANCA-MPO patients (D). MCD patients show extensive DNase I expression compared to the tubulo-interstitium of patients with ANCA-MPO. Negative control for antibody specificity confirms the significant diminution of DNase I in MPO-ANCA GN. *P<0.05, ****P<0.0001 Data are means ± SEM Human Data is from *n*=29 (MPO-ANCA GN) and *n*=6 (MCD) in each group and analyzed by Mann-Whitney U. MPO, myeloperoxidase, ANCA anti neutrophil cytoplasmic antibody, GN, glomerulonephritis, Ctrl, Control; DNase I, Deoxyribonucleic I; dsDNA, double stranded deoxyribonucleic acid, ecDNA, extracellular deoxyribonucleic acid. Original magnification 400x, HP inset 3000x.

Figure 2. Mice with autoimmune anti-MPO GN have significantly enhanced renal deposition of ecDNA and diminution of DNase I, which is attenuated by ivDNase I. (A) Experimental timeline showing three groups of mice immunized with MPO (*n*=12) or ovalbumin (n=6) followed by injection with 3mg anti-GBM Ig on Day 16. MPO-immunized mice then received twice daily injections of saline (*n*=6) or ivDNase I (*n*=6). (B) Representative kidney sections from mice immunized with OVA, MPO or MPO-immunized mice that were later treated with ivDNase I. Sections were stained for ecDNA (red) and counter-stained with β actin (green). (C) Semi-quantitation of ecDNA in kidney sections

made from OVA (1), MPO (2) and MPO-immunised ivDNase I-treated groups (3) was performed using Image J and the amount of ecDNA is expressed as arbitrary units per glomerular cross section (AU/gcs). (D) Histological scoring of the tubulointerstitium of mouse kidneys for DNase I with x-axis depicted the same as (C) (E) Representative images of DNase I immunohistochemistry across experimental groups. *P<0.05, **P<0.01. Data are mean ± SEM from six mice in each group analyzed by Mann-Whitney U or Kruskal- Wallis, for 3 or more groups. Abbreviations: MPO, myeloperoxidase, ANCA anti neutrophil cytoplasmic antibody, GN, glomerulonephritis, Ctrl, Control; DNase I, Deoxyribonuclease I; ecDNA, extracellular deoxyribonucleic acid; dsDNA, double stranded deoxyribonucleic acid ;OVA, Ovalbumin. Original magnification 400x.

Figure 3. **DNase I treatment reduces histological glomerular injury, leukocyte recruitment and functional injury in experimental MPO-ANCA GN.** Disease was induced in animals that were then treated with ivDNase I or saline. Animals were assessed for the following parameters. (A) percentage of abnormal gloumeruli in MPO-ANCA with DNase I quantitated after assessment of (B) murine kidney sections stained with periodic acid-Schiff, (C) percentage of gloumeruli containing fibrin that was quantitated after assessment of (D) murine kidney sections treated with fibrin antibody?. Glomeruli were also assessed by immunoperoxidase-staining for (E) CD4+ T cells, (F) macrophages and (G) neutrophils. (H) Presence of albumin in the urine of mice collected over 24 hours. Animals were also assessed for (I) Dermal delayed hypersensitivity response in an MPO footpad challenge, (J) frequency of MPO-specific IFNγ and (K) frequency of MPO-specific IL17A producing cells in lymph nodes draining sites of MPO immunization. *P<0.05, **P<0.01. Data are mean ± SEM from six mice in each group analyzed by Mann-Whitney U. Anti MPO-ANCA GN, Anti Myeloperoxidase Anti Neutrophil Cytoplasmic Antibody Glomerulonephritis; MPO,

myeloperoxidase; DNase I, Deoxyribonuclease I; Ctrl, Control; DNase I, Deoxyribonuclease I; Original Magnification 600x.

Figure 4. **DNase I treatment reduces NET formation and deposition of extracellular MPO in established anti-MPO-ANCA GN**. (A) Kidney sections from ANCA-MPO GN mice receiving either saline control or ivDNase I treatment stained for NETS as seen by co-localisation of MPO (red), H3Cit (green), PAD4 (white) and DAPI (blue) indicated by arrows, and deposits of MPO indicated by arrow heads. (B) NETS quantitation in glomeruli of ivDNase I treated and control ANCA-MPO GN animals. (C) Kidney sections labelled for MPO (red), CD45 (green) and DAPI (blue) were assessed for intracellular MPO (co-localisation of CD45 and MPO, arrow head) and extracellular MPO (non-co-localised CD45 and MPO, arrows). (D) Extracellular MPO quantitation in glomeruli of ivDNase I treated and control ANCA-MPO GN animals. **$P<0.01$. Data are mean ± SEM from six mice in each group analyzed by Mann-Whitney U. Anti MPO-ANCA GN, Anti Myeloperoxidase Anti Neutrophil Cytoplasmic Antibody Glomerulonephritis; MPO, myeloperoxidase; DNase I, Deoxyribonuclease I; Ctrl, Control PAD4, peptidylarginine deiminase; H3Cit, Citrullinated Histone 3; DAPI, 4', 6- diamidino-2-phenylindole, Ctrl, Control; DNase I, Deoxyribonuclease I; CD45, pan leukocyte marker C45. Original Magnification 600x

Figure 5. DNase I treatment given during and after establishment of autoimmunity to MPO reduces systemic anti-MPO autoimmunity. (A) Experimental timeline for a 10-day MPO immunization model where mice receive saline of ivDNase I one day prior to immunization with MPO. Mice subsequently receive saline or ivDNase I every day until termination of the experiment at ten days post-immunization. Animals were assessed for (B) delayed type hypersensitivity response to an MPO challenge in the footpad, (C) anti-MPO antibodies and frequency of (D) MPO-specific IFNγ, (E) MPO-specific IL17A and (F) CD4 T regulatory cells in lymph nodes draining sites of MPO immunization. (G) Experimental timeline for an 18-hour model MPO immunization model

where mice receive saline of ivDNase I one day prior to immunization with MPO with experiment terminated 18 hours post-immunization. The lymph nodes draining the site of MPO immuinization site were assessed for the frequency of (H) CD11c dendritic cells that also expressed (I) CD80, (J) CD86, (K) OX40L, (L) CD40, (M) ICOS or (N) MHC II. (O) Frequency of activated CD4 T cells in lymph nodes draining the site of MPO immuinization. *P<0.05, **P<0.01, ***P<0.001, analyzed by Mann-Whitney U. Data are mean ± SEM from n=10 mice in the 10-day model and n=8 mice in the 18-hour model.. D-1, day minus 1; FCA, Freunds Complete Adjuvant; µg, micrograms; kg, Kilograms; IV, intravenous tail injection; DTH, Delayed Type Hypersensitivity MPO, myeloperoxidase; IFNγ, Interferon gamma; IL-17A, Interleukin 17A, ELISPOT, Enzyme-Linked ImmunoSpot; DNase I, Deoxyribonuclease I; Ctrl, U. FACS, Fluorescence-activated cell sorting; CD80, Cluster of differentiation; CD86, Cluster of differentiation 86; CD40, Cluster of differentiation 40 (co- stimulatory molecules); OX40L, CD252 (marker of activation); ICOS, Inducible T-cell co- Stimulator; MHCII, major histocompatibility complex; CD69, Cluster of differentiation 69 (marker of T cell antigen activation). DNase I, Deoxyribonuclease I; Ctrl, Control.

Figure 6. Extracellular DNA is reduced in DNase I-treated mice in a passive transfer model of ANCA-dependent anti-MPO GN. (**A**) Experimental timeline of a second model for ANCA-MPO GN where mice receive saline or ivDNase I 1-day prior to receiving LPS and anti-MPO IgG (B) Kidney sections from mice receiving either saline control or ivDNase I treatment stained for DNA (red) and b-actin (green) were assessed were quantitatively assessed using Image J for (C) ecDNA (expressed in arbitrary units) per glomeruli cross-section. (**D**) Histological scoring of the tubulointerstitium of mouse kidneys for DNase I was performed on (**F**) kidney sections immunohistochemically-labelled for DNase I. *P<0.05, ***P<0.001. Data are mean ± SEM from six mice in each group analyzed by Mann-Whitney U or Kruskal-Wallis for 3 or more groups. Abbreviations: Ctrl, Control; DNase I, Deoxyribonuclease I; ecDNA, extracellular deoxyribonucleic acid. Original magnification 400x

Figure 7. NET formation is abolished by DNase I treatment in a passive ANCA-dependent model of anti-MPO GN.

(A) Kidney sections from passive ANCA-MPO GN mice receiving either saline control or ivDNase I treatment stained for NETS as seen by co-localisation of MPO (red), H3Cit (green), PAD4 (white) and DAPI (blue) indicated by arrows (B) NETS quantitation in glomeruli of ivDNase I treated and control passive ANCA-MPO GN animals. (C) Kidney sections labelled for MPO (red), CD45 (green) and DAPI (blue) were assessed for intracellular MPO (co-localisation of CD45 and MPO) and extracellular MPO (non-co-localised CD45 and MPO, arrows). (D) Extracellular MPO quantitation in glomeruli of ivDNase I treated and control passive ANCA-MPO GN animals. *P<0.05, ***P<0.001. Data are means ± SEM from six mice in each group analyzed by Mann-Whitney U. MPO, myeloperoxidase: PAD4, peptidylarginine deiminase; H3Cit, Citrullinated Histone 3; DAPI, 4', 6-diamidino-2-phenylindole, Ctrl, Control; DNase I, Deoxyribonuclease I; CD45, pan leukocyte marker C45. Original Magnification 600x

Figure 8. DNase I treatment reduces glomerular injury in a passive ANCA-dependent model of anti-MPO GN. Kidney sections from animals receiving saline-control or DNase I-treatment after passive ANCA-induced anti-MPO-GN were enumerated for evidence of functional glomerular injury as seen by (A-B) abnormal glomeruli (C-D) polymorphonucleocyte infiltration (E-F) macrophage infiltration (G-H) CD4-T cell infiltration and (**I**) 24 hour albuminuria levels. *P<0.05, ** P<0.01, ***P<0.001. Data are mean± SEM from six mice in each group analyzed by Mann- Whitney U. Ctrl, Control; DNase I, Deoxyribonuclease I. Original Magnification 400x.

Figure 9. DNase I treatment in a passive ANCA-mediated model of anti MPO-GN reduces mRNA production of kidney inflammatory markers and DNase I. RNA was extracted from the kidneys of animals receiving saline-control or DNase I-treatment after

passive ANCA-induced anti-MPO-GN and assessed by qRT-PCR for (A) CCL2, (B) CXCL1, (C) CXCL2, (D) IFN-□, (E) IL-1□, (F) IL-6, (G) TNF□, (H) DNase I. Values are normalized to 18S ribosomal RNA. *P<0.05, ** P<0.01, ***P<0.001. Data are means± SEM from six mice in each group analyzed by Mann-Whitney U. Ctrl, Control; DNase I, Deoxyribonuclease I.

Figure 10. AdAV-DNase I treatment is superior to exogenously administered DNase I in reducing autoimmunity to MPO in the 20-day ANCA anti-MPO GN model. (A) Vector constructs used in the (B) the 20-day ANCA model were assessed for C) serum DNase I activity levels. (D) After completion of the experiment, mice were assessed for footpad delayed type hypersensitivity response in response to MPO, (E) MPO ANCA levels, and the frequency of anti-MPO reactive cells in the lymph nodes that drained the site of MPO immunization that secreted (F) IFN-g or (G) IL-17A. *P<0.05, ** P<0.01, ***P<0.001. Data are mean± SEM from (n=8 mice per group) analyzed by Mann-Whitney U. AdAV, Adeno associated viral vector; ANCA, anti- neutrophil cytoplasmic antibody; Ctrl, Control; DNA, Deoxyribonucleic acid; DNase I, Deoxyribonuclease I;GFP, green fluorescent protein; H3Cit, Citrullinated Histone 3;MPO, myeloperoxidase.

Figure 11. AdAV-DNase I treatment reduces kidney injury, glomerular leukocytes infiltration, cell death and NETosis. Treatment with AdAV-DNase I significantly reduces 24-hour albuminuria (**A**) and significantly reduces histological glomerular injury compared to both the control GFP vector and endogenously administered DNase I (**B**). Glomerular leukocyte recruitment is significantly reduced in mice treated with both the exogenous DNase I and AdAV-Dnase I vector when compared to the control AdAV- GFP vector (**C-E**). Representative figures of a reduction in both segmental necrosis and markers pf cell death RIPK3 and Caspase 3 are reduced in mice treated with the AdAV-DNase I vector compared to the control AdaV-GFP vector (**F**). Neutrophil NET assays stimulated with PMA and treated with DNase I at 4ug/ml demonstrate attenuation of NETs, with DNA observed in blue, MPO

in red, H3Cit in green and PAD4 in grey/blue (**G**). Zymosan phagocytosis assays with neutrophils incubated with DNase I at increased concentrations (blue dots) show that DNase I does not inhibit neutrophil phagocytosis when compared to positive control (red dots) (**H**). *P<0.05, ** P<0.01, ***P<0.001. Data are means± SEM from 8 mice in each group analyzed by Mann-Whitney U. AdAV, Adeno associated viral vector;Ctrl, Control; DNA, Deoxyribonucleic acid; DNase I, Deoxyribonuclease I;GFP, green fluorescent protein; H3Cit, Citrullinated Histone 3;MPO, myeloperoxidase; PAD4, Peptidyl arginine deiminase 4, PMA, Phorbal myristate acetate

Supplementary Table of Contents (submitted as separate PDF) Supplementary Figure Legends

Supplementary Table 1. Clinical Data from patients with ANCA associated Vasculitis

Supplementary Figure 2. Subnephritogenic anti GBM Ig does not induce injury alone

Supplementary Figure 3. Mice immunized with an irrelevant antigen OVA do not develop autoimmunity to MPO shown by lack of development of humoral and cellular responses to MPO at 10 days or 20 after first immunisation with OVA

Supplementary Tables

Table 1. Clinical Data from patients with ANCA associated Vasculitis

Patient Characteristics	**MPO-AAV**	**MCD**
Patient number	29	6
Age	63.53 (±3)	
Sex F/M	15/14	4/2
Number of glomeruli	18.35.7 (±2)	19
Laboratory values		
MPO-ANCA titre (U/ml)	149.58 (±231)	n/a
eGFR (ml/min per 1.73 m^2)	34.77 (±8)	100.1 (±6)
ESR (mm/h)	70 (±8)	n/a
CRP (mmol/l)	66.47 (±25)	n/a
Red blood cells (cells/HPF)	552 (±151)	n/a

Abbreviations: ANCA, anti-neutrophil cytoplasmic antibody; CRP, C reactive protein; eGFR, estimated glomerular filtration rate; ESR, erythrocyte sedimentation rate;MCD, minimal change disease MPO, myeloperoxidase

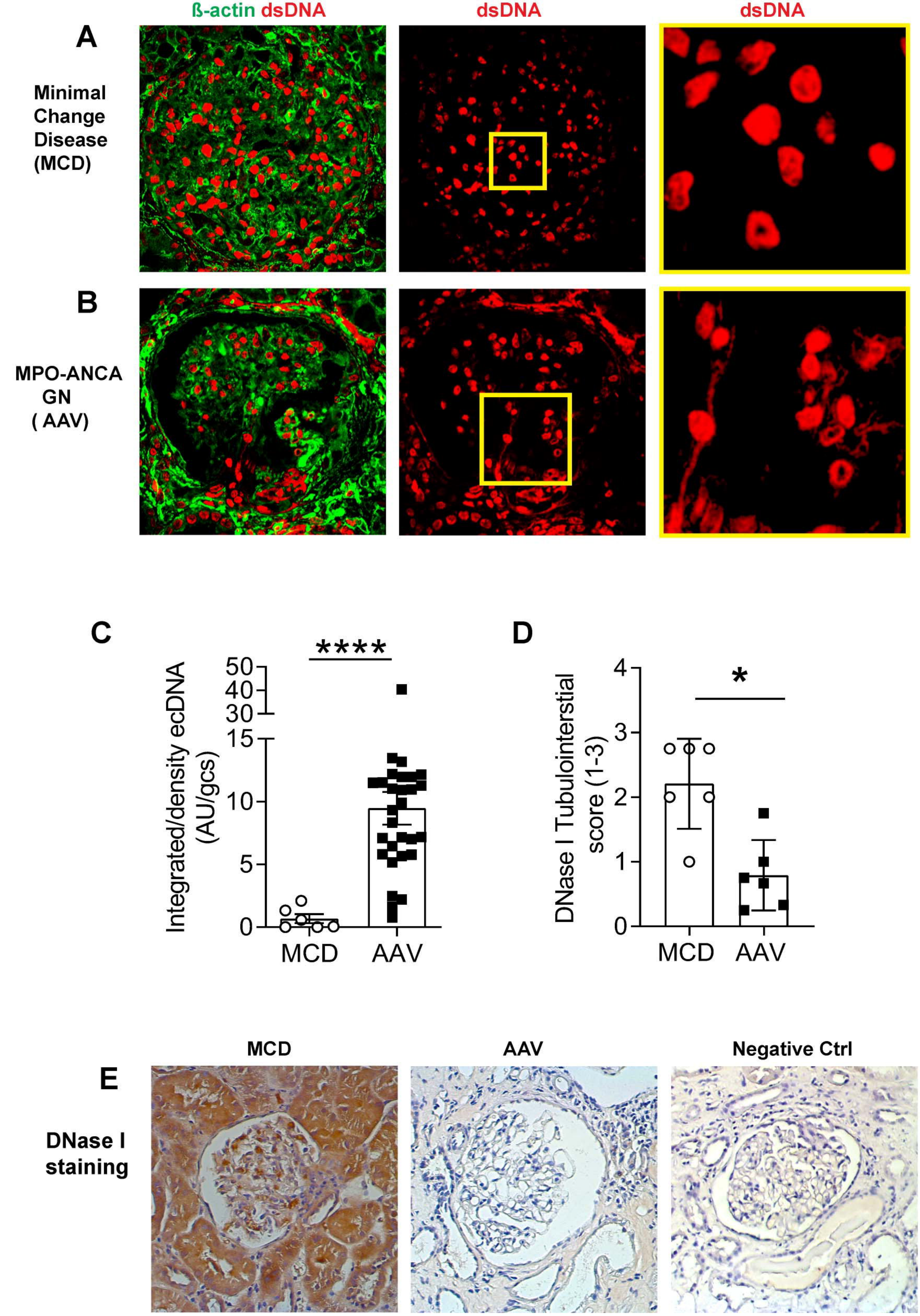

Figure. 1 Enhanced extracellular DNA deposition and reduced DNase I expression is seen in kidney biopsies from patients with MPO-ANCA GN (AAV)

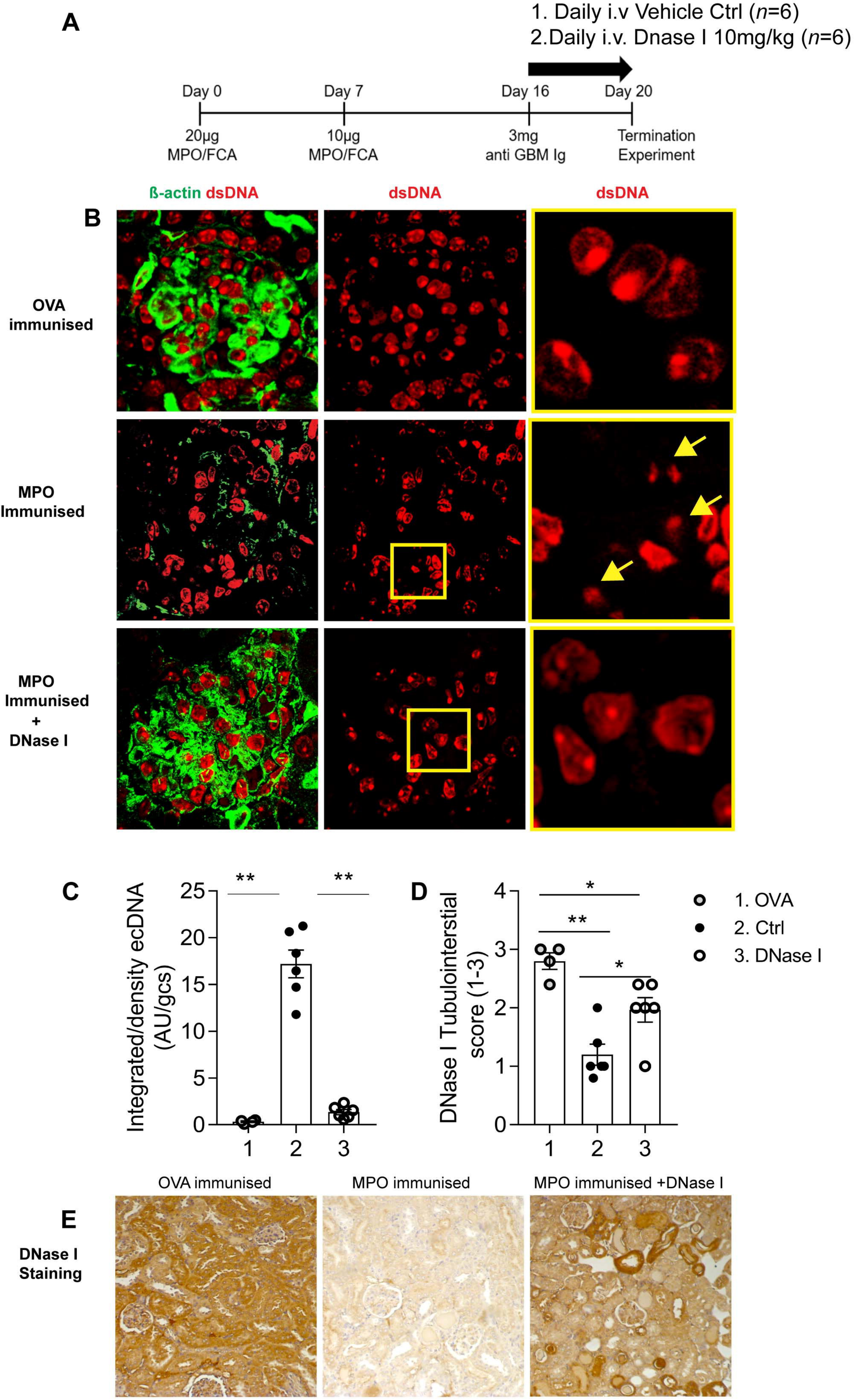

Fig. 2 Mice with autoimmune anti MPO GN have significantly enhanced renal deposition of ecDNA and diminution of DNase I which is attenuated by ivDNase I

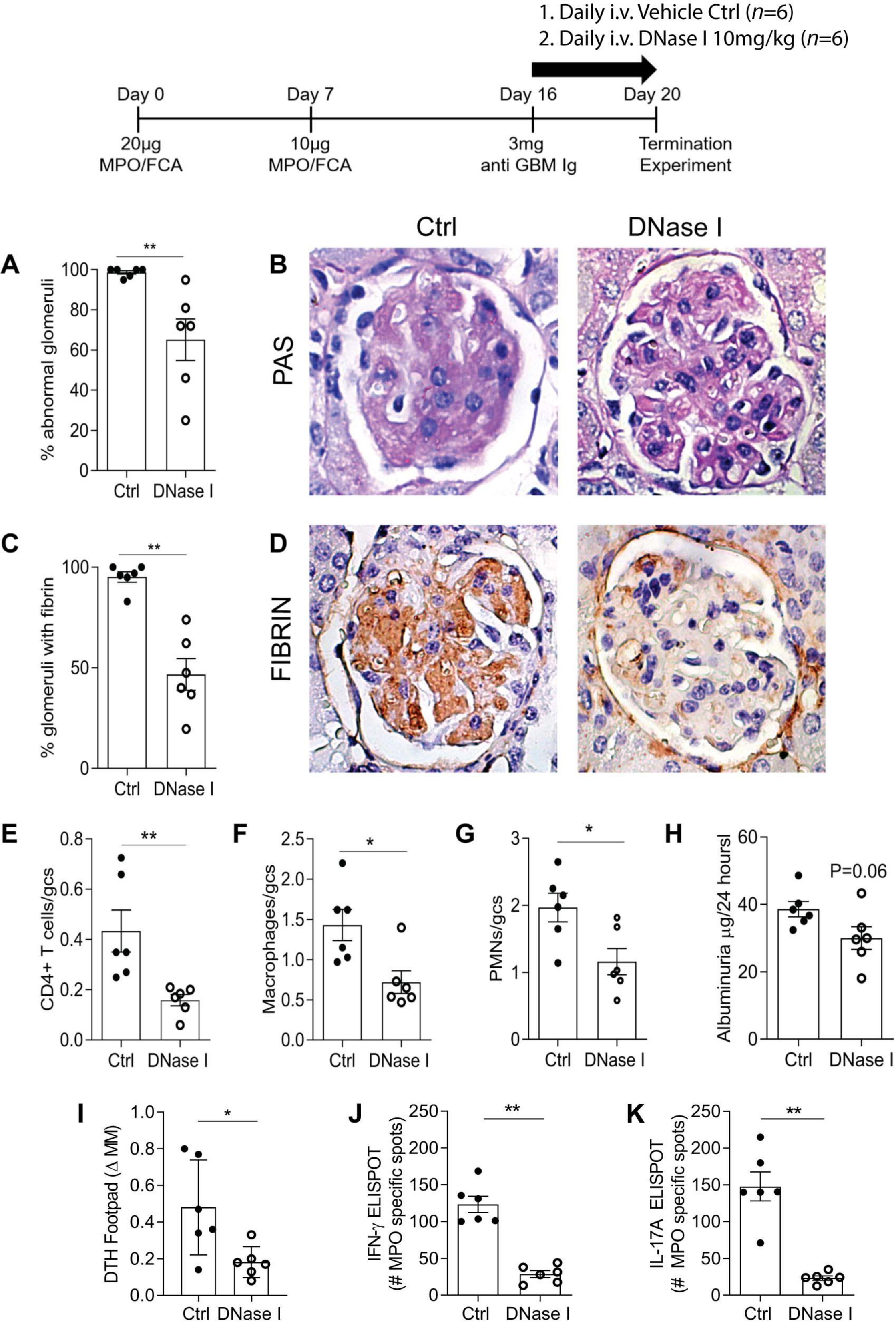

Figure 3. Dnase I treatment reduces histological glomerular injury, leukocyte recruitment functional injury and autoimmunity to MPO in experimental anti MPO GN

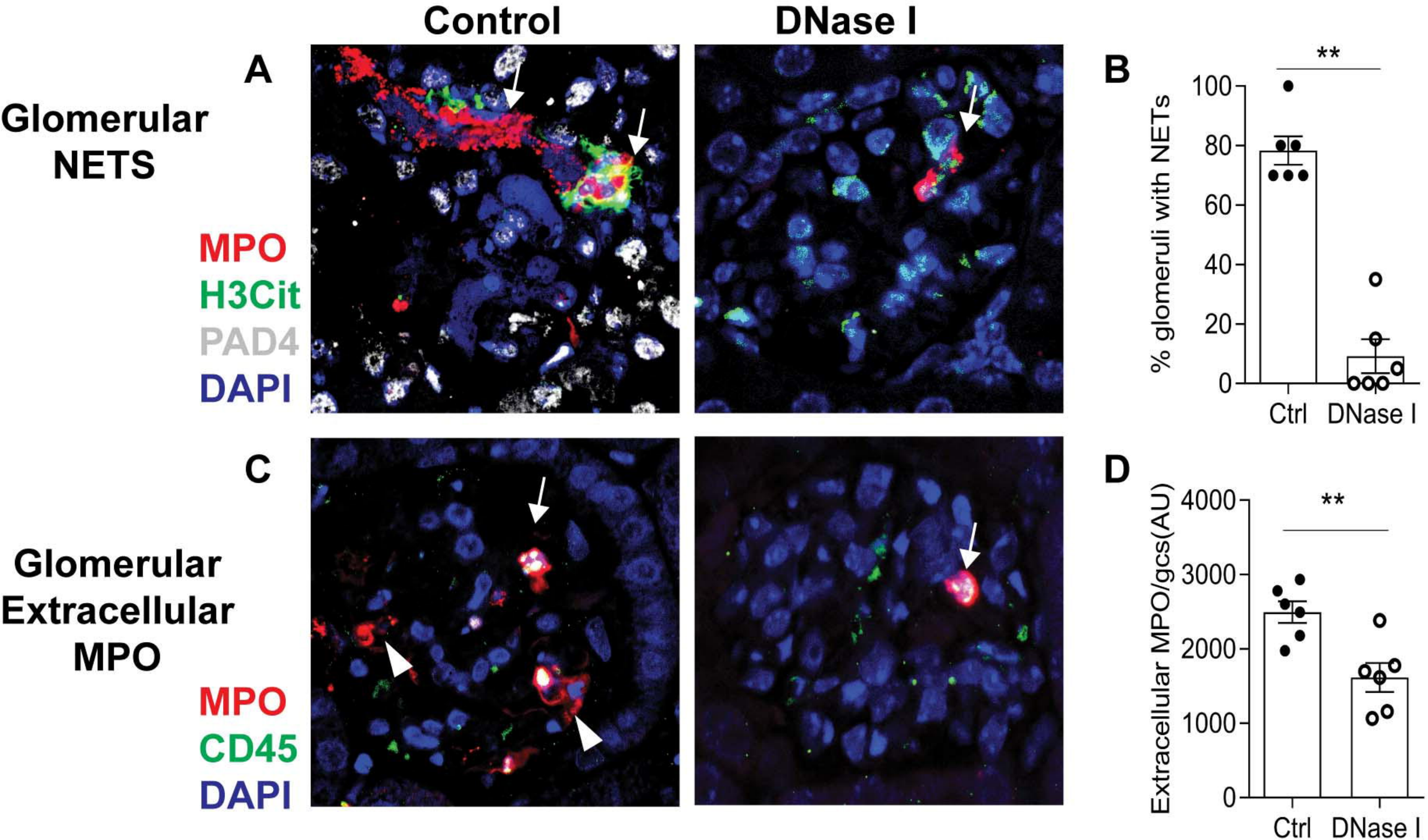

Figure 4. DNase I treatment reduces NET formation and deposition of extracellular MPO in established anti MPO-ANCA GN.

DNase I treatment attenuates the development of MPO autoimmunity

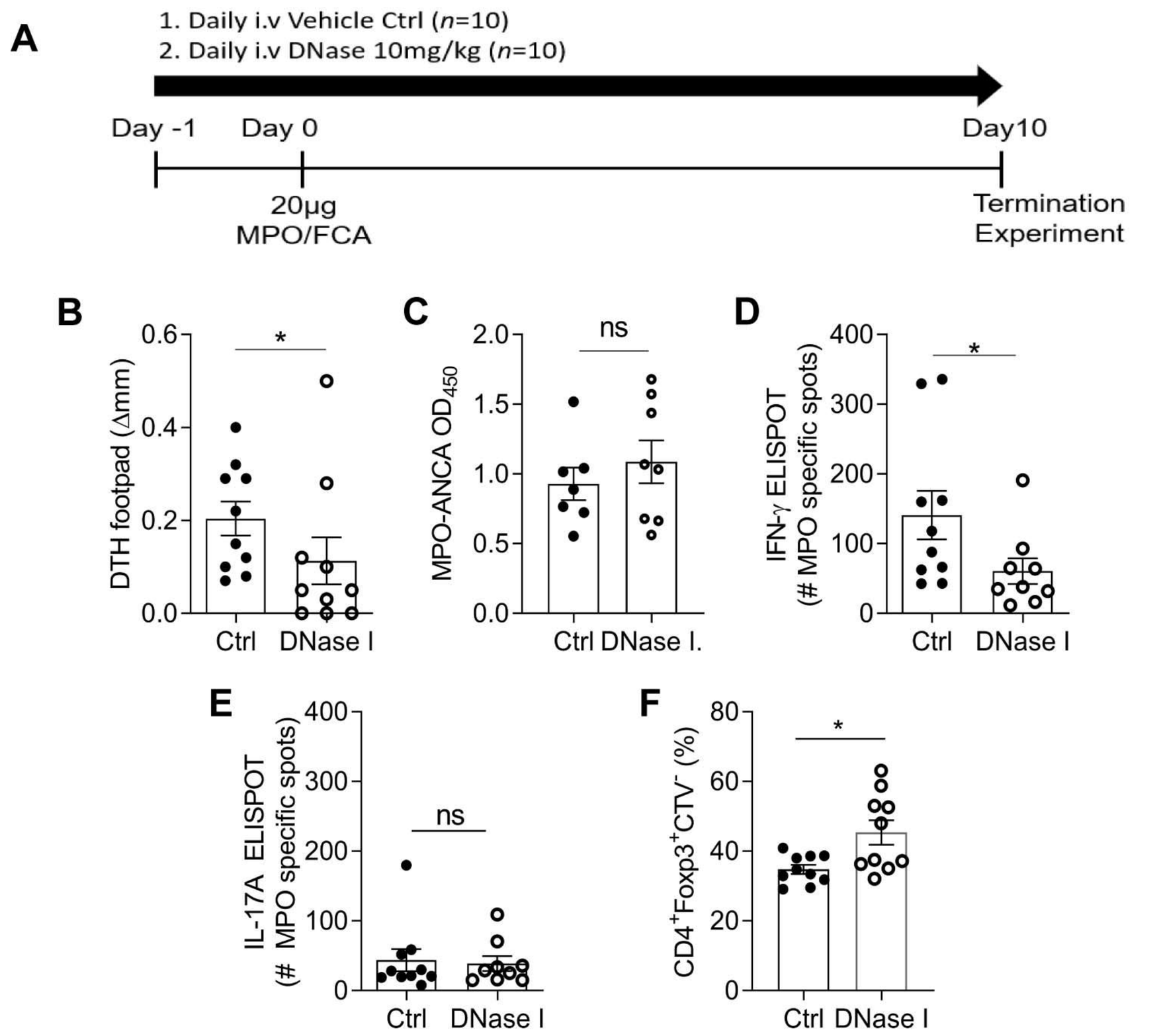

DNase I inhibits DC migration and activation from the draining lymph nodes

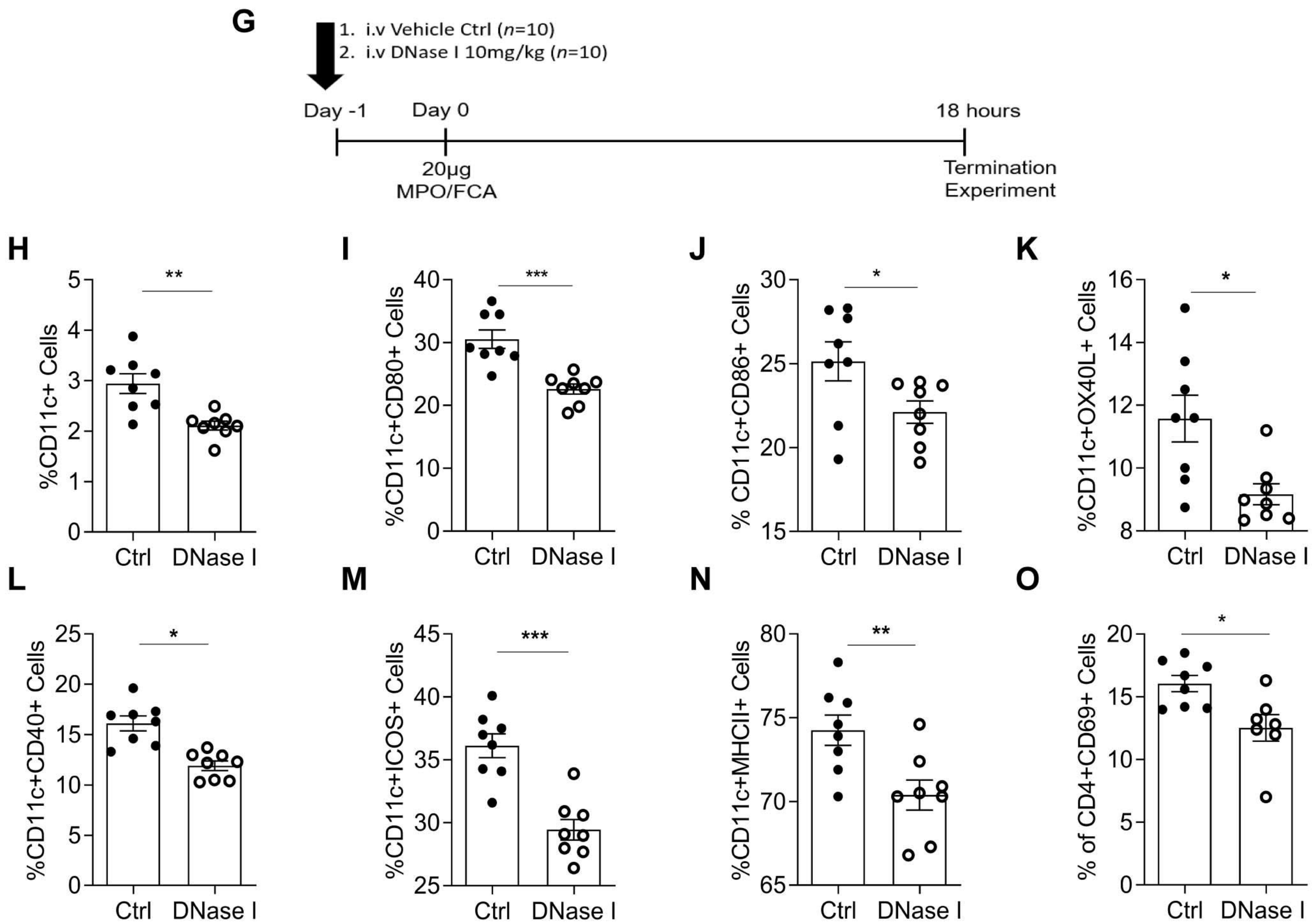

Fig. 5 DNase I treatment reduces autoimmunity to MPO and reduces Dendritic Cell and T cell activation in the draining lymphnodes

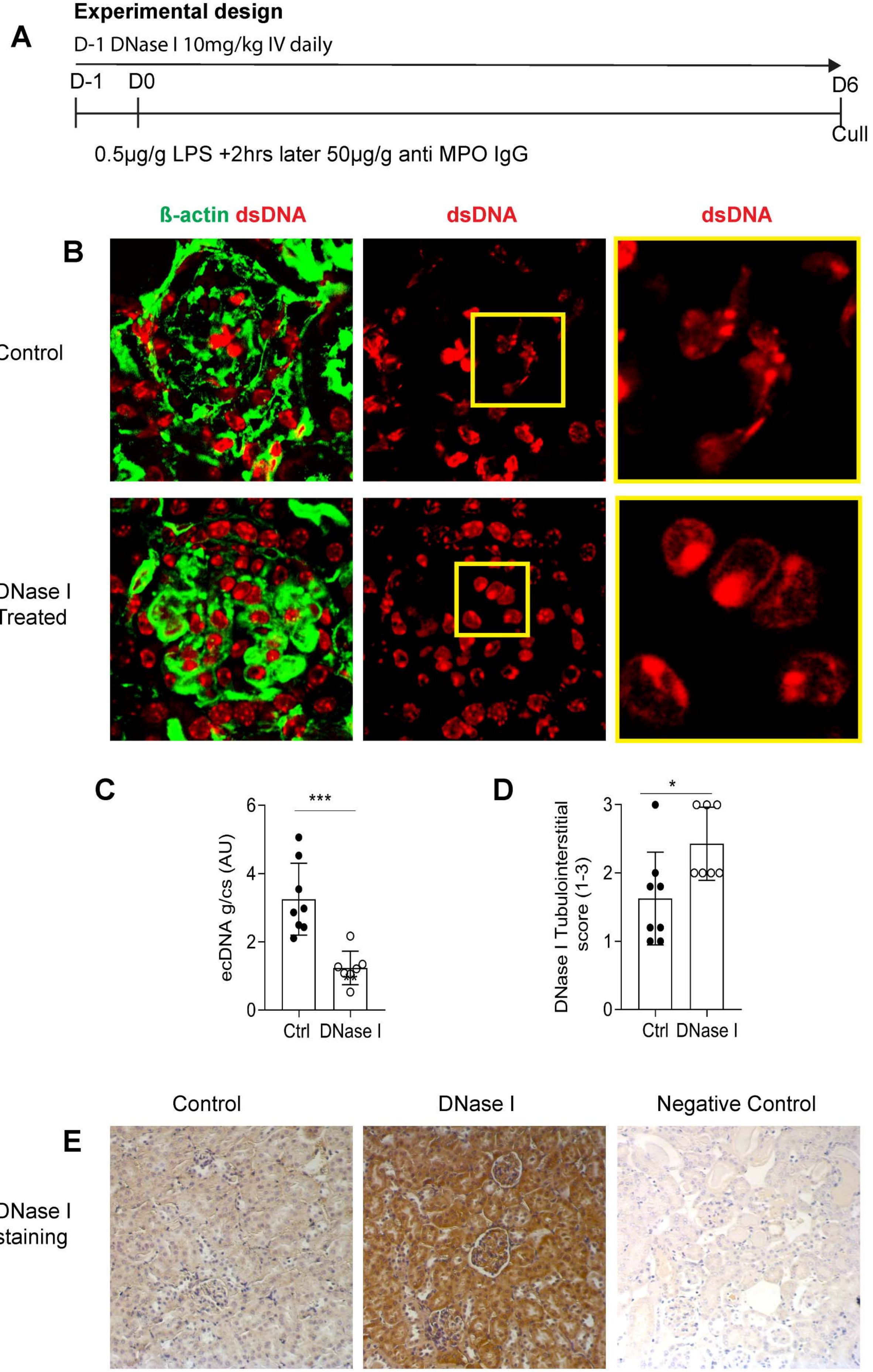

Figure 6. Extracellular DNA is a prominent feature in an ANCA dependent model of anti-MPO GN

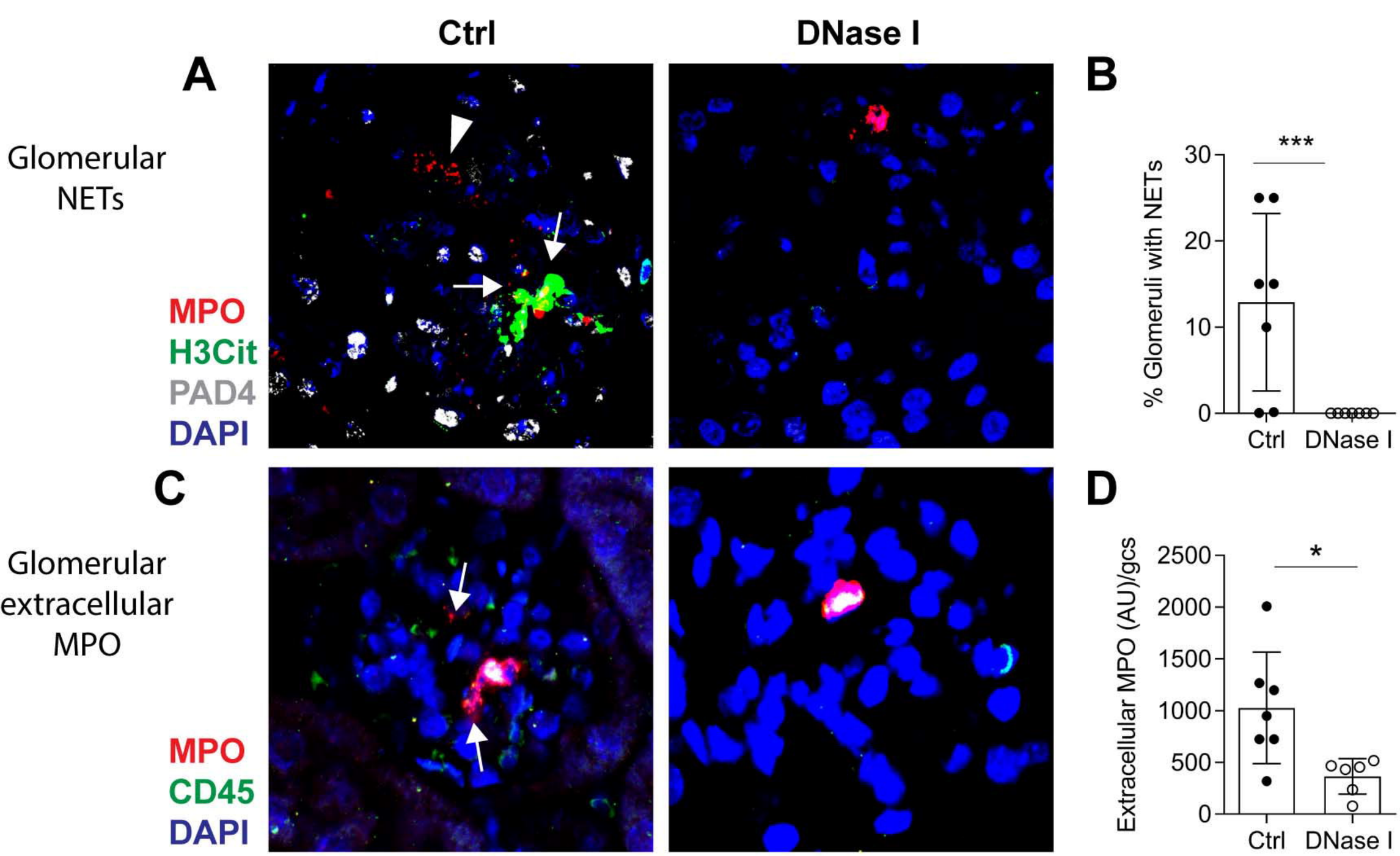

Figure 7. NET formation is abolished in an ANCA dependent model of anti MPO-GN

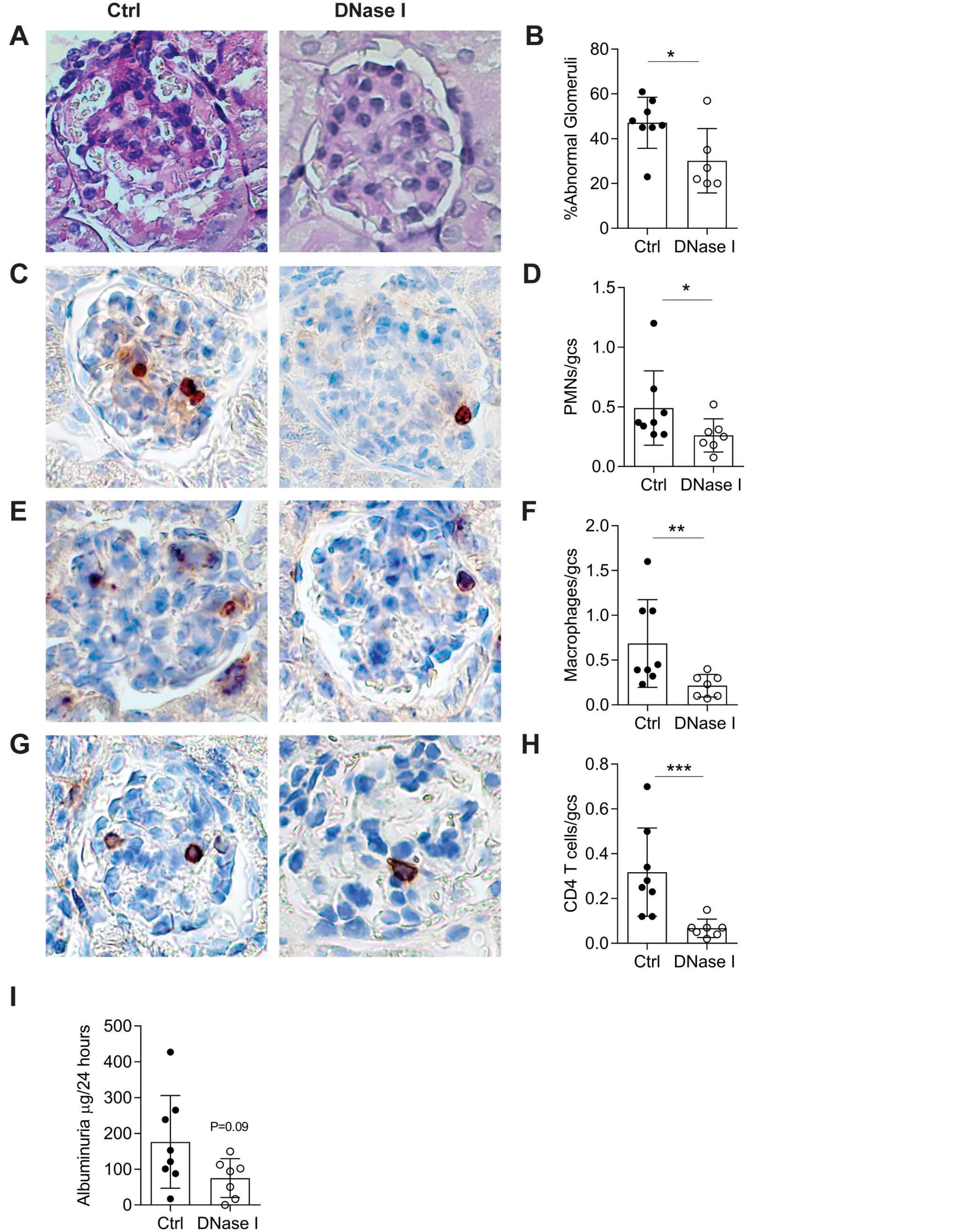

Figure 8. DNase I treatment reduces glomerular injury in an ANCA mediated model of anti-MPO GN

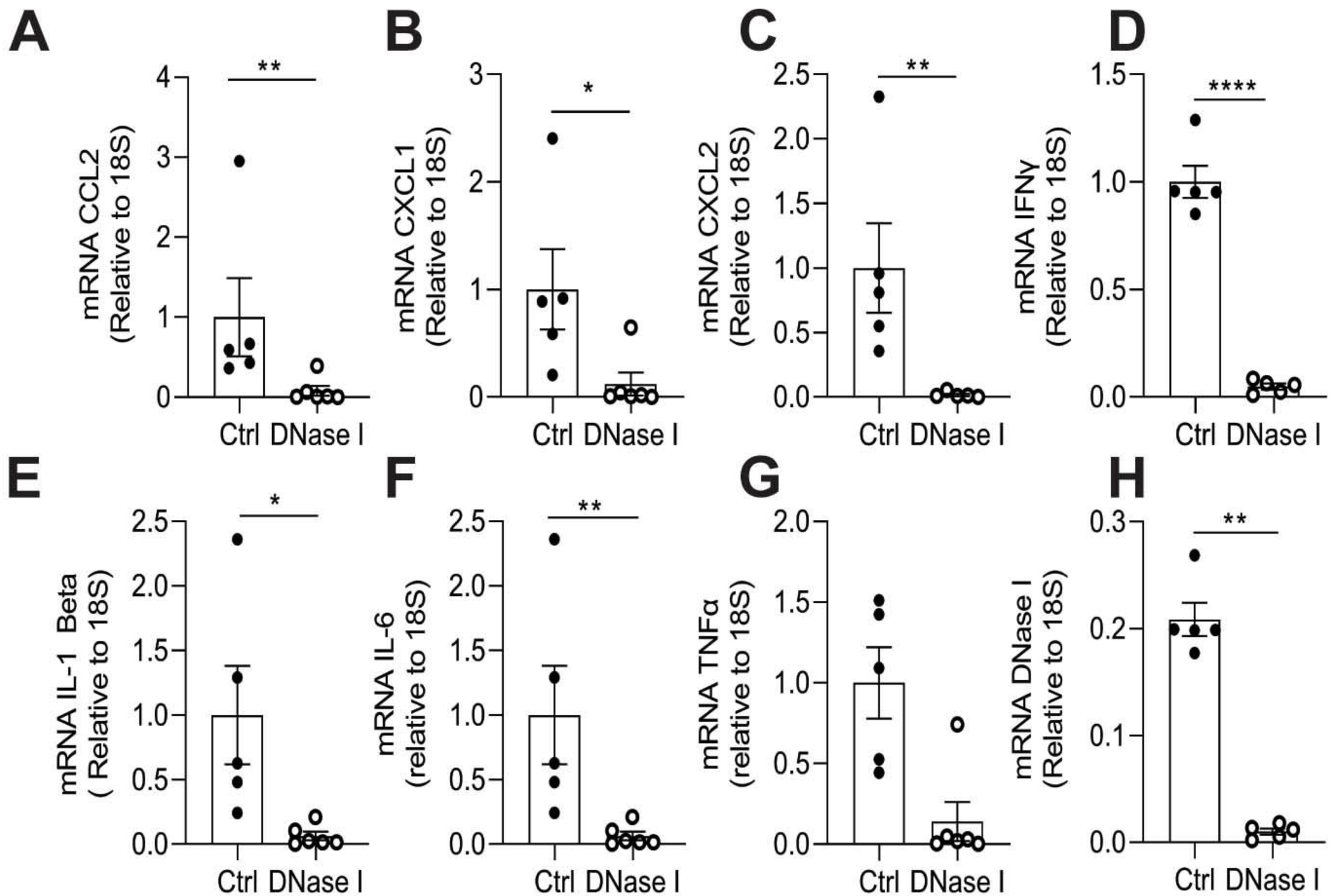

Fig.9 . DNase I treatment in a passive ANCA-mediated model of anti MPO-GN reduces mRNA production of kidney inflammatory markers and DNase I.

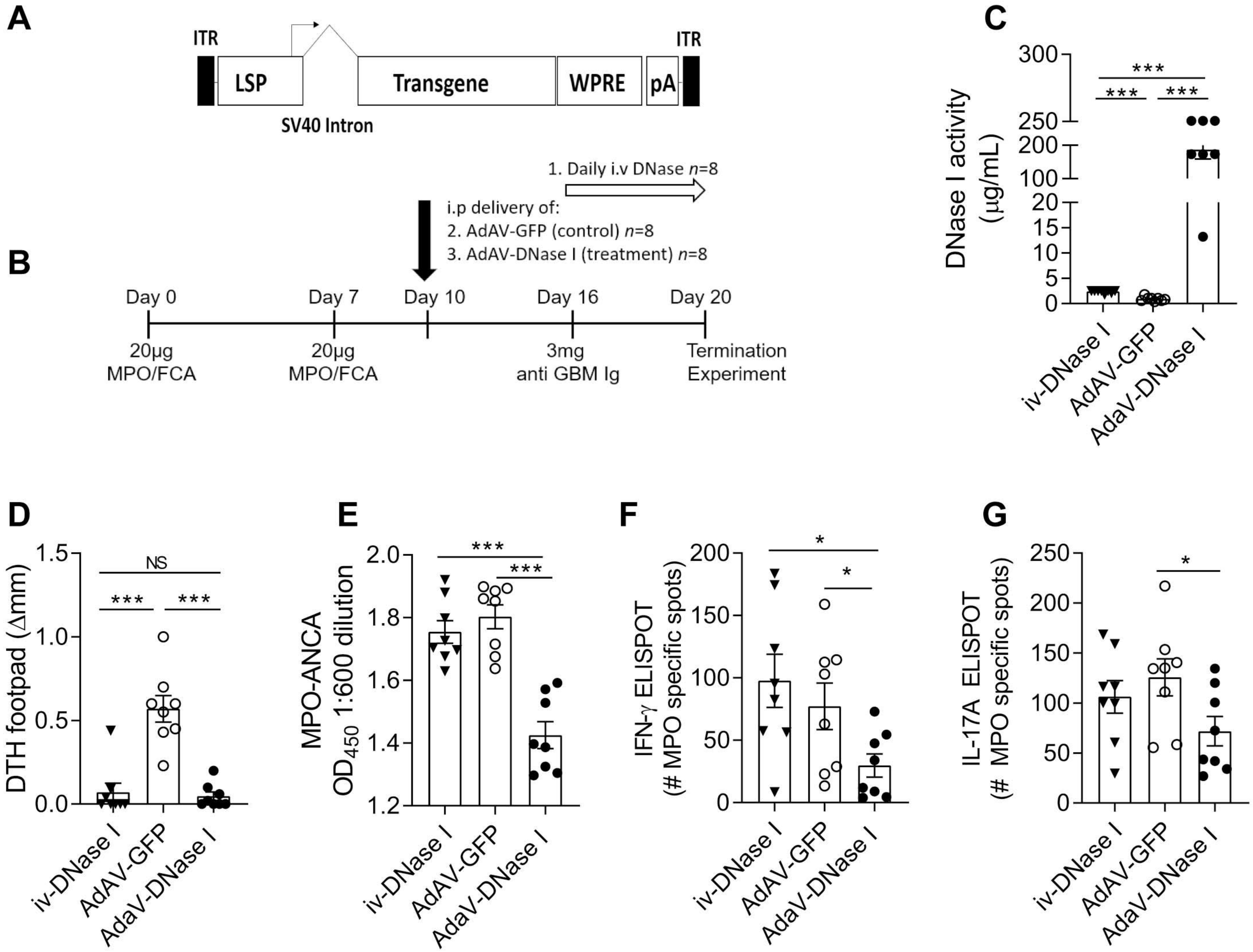

Figure. 10 AdAV-DNase I treatment is superior to exogenously administered DNase I in reducing autoimmunity to MPO in the 20-day ANCA anti-MPO GN model